

**INTELLIGENT SMART RESTORATION TECHNIQUE FOR
MICROGRIDS**

BY

MD. ILIUS HASAN PATHAN

A Thesis Presented to the
DEANSHIP OF GRADUATE STUDIES

KING FAHD UNIVERSITY OF PETROLEUM & MINERALS

DHAHRAN, SAUDI ARABIA

In Partial Fulfillment of the
Requirements for the Degree of

MASTER OF SCIENCE

In

ELECTRICAL ENGINEERING

DECEMBER 2017

KING FAHD UNIVERSITY OF PETROLEUM & MINERALS

DHAHRAN- 31261, SAUDI ARABIA

DEANSHIP OF GRADUATE STUDIES

This thesis, written by **MD. ILIUS HASAN PATHAN** under the direction of his thesis advisor and approved by his thesis committee, has been presented and accepted by the Dean of Graduate Studies, in partial fulfillment of the requirements for the degree of **MASTER OF SCIENCE IN ELECTRICAL ENGINEERING.**



Dr. Ali Ahmad Al-Shaikhi
Department Chairman



Dr. Mohammad M. Al-Muhaini
(Advisor)



Dr. Ibrahim Mohamed ElAmin
(Member)



Dr. Salam A. Zummo
Dean of Graduate Studies



Dr. Ibrahim O. Habiballah
(Member)

28/12/17
Date

© Md. Ilius Hasan Pathan

2017

|Dedicated To My Parents |

ACKNOWLEDGMENTS

|

At first, I would like to express my gratitude towards the almighty ALLAH for giving me chance and ability to attain this thesis. I am also thankful to Prophet (Sallallahu alaihe wasallam) for giving the message about ALLAH that nothing is possible without His mercy and blessing.

I would like to express my gratefulness to my advisor, Dr. Mohammad Al-Muhaini for his continuous guidance and encouragement, and valuable suggestions all through. He taught me the way to overcome the impediment of research works with staunchness and diligence.

I shall also ever remain thankful to my all course teachers for their enlightened teaching.

I would like to thank my thesis committee members, Dr. Ibrahim M. El-Amin and Dr. Ibrahim O. Habiballah, for being supportive too.

I am also grateful to Maad AlOwaifeer and Abass Afolabi Yahaya for their valuable suggestions and providing necessary documents for this thesis.

Last, but certainly not least, I am immensely indebted and thankful to my parents, brothers, and relatives, in persons of my elder brother, Engr. Md. Imran Hasan Pathan, for their unremitting love, psychological support and encouragement all through of my higher study. |

TABLE OF CONTENTS

ACKNOWLEDGMENTS	V
TABLE OF CONTENTS	VI
LIST OF TABLES	IX
LIST OF FIGURES	X
LIST OF ABBREVIATIONS	XI
ABSTRACT	XIII
ملخص الرسالة	XV
CHAPTER 1 INTRODUCTION	1
1.1 Electric Microgrid	1
1.2 Motivation	2
1.3 Objectives	4
1.4 Contribution of this Thesis	5
1.5 Thesis Organization	5
CHAPTER 2 LITERATURE REVIEW	7
2.1 Impact of Distributed Generators on Distribution Networks	7
2.2 Demand Side Management	10
2.3 Placement and Sizing of DG for Reliability Improvement	12
2.4 Network Reconfiguration Technique	14
2.5 Restoration Priority Listing	17

CHAPTER 3 SYSTEM MODELING AND MODEL EVOLUTION	23
3.1 Forecasting Technique Modeling	23
3.1.1 Fuzzy Time Series-Markov Chain Model	24
3.1.2 Implementation of Fuzzy Time Series-Markov Chain Model	30
3.2 Photovoltaic (PV) DG Model	33
3.3 Wind DG Model	38
3.4 Load Model	40
3.5 Storage System Model	43
3.5.1 Modeling Charging-Discharging Procedure of Storage	43
3.5.2 Fuzzy Decision-Making Technique	50
3.5.3 Calculation of Transition Probabilities	51
3.5.4 Transition Matrix and Limiting Probabilities	53
3.5.5 Availability Calculation	54
3.5.6 Storage Sizing	54
CHAPTER 4 PROBLEM FORMULATION AND METHOD	58
4.1 Objective Function Formulation	58
4.2 Constraints	60
4.3 Genetic Algorithm	62
4.3.1 Selection	62
4.3.2 Crossover	62
4.3.3 Mutation	63
CHAPTER 5 RESULTS AND CONCLUSION	64
5.1 Test System	64
5.2 Type and Number of Consumers	65

5.3	Proposed Algorithm for Distribution Network Restoration	66
5.4	Case Studies	68
5.4.1	Case 1	69
5.4.2	Case 2	72
5.4.3	Case 3	75
5.4.4	Case 4	78
CHAPTER 6 CONCLUSIONS AND FUTURE WORK		82
6.1	Conclusions	82
6.2	Future Work	83
REFERENCES		84
VITAE		95
APPENDIX A		96
APPENDIX B		97

LIST OF TABLES

Table 3.1: Sample Historical Values & Fuzzification	29
Table 3.2: 5-Parameter Model Output and CS6X-320P Datasheet Specification	37
Table 3.3: Wind Turbine Parameters	39
Table 3.4: Transition Probability	52
Table 5.1: Consumer Types, Numbers and Connecting Bus Information	65
Table 5.2: List of Case Study.....	68
Table 5.3: Load Values of 33 Buses at 753 th & 754 th Hours	69
Table 5.4: Results of IEEE 33 Bus Using Tournament Selection	70
Table 5.5: Results of IEEE 33 Bus Using Random Selection	71
Table 5.6: Results of IEEE 33 Bus Using Tournament Selection	73
Table 5.7: Results of IEEE 33 Bus Using Random Selection	74
Table 5.8: Load Values of 33 Buses at 3585 th & 3586 th Hours	75
Table 5.9: Results of IEEE 33 Bus Using Tournament Selection	76
Table 5.10: Priority List for Buses.....	77
Table 5.11: Results of IEEE 33 Bus Using Tournament Selection	79

LIST OF FIGURES

Figure 3.1: Fuzzy Time Series-Markov Chain State Transition Diagram	26
Figure 3.2: Histogram of Hourly Daytime & Nighttime Temperature of One Year	31
Figure 3.3: Histogram of Hourly Daytime & Nighttime Radiation of 1 st Season	31
Figure 3.4: Histogram of Hourly Daytime & Nighttime Radiation of One Year	32
Figure 3.5: Histogram of Hourly Wind Speed of One Year	33
Figure 3.6: 5-Parameter Model Equivalent Circuit.....	34
Figure 3.7: Hourly PV Power Output for a Year Using 5-Parameter Model	38
Figure 3.8: Hourly Wind Power Output for a Year	40
Figure 3.9: Hourly Total Residential Load for a Year on Distribution Network	42
Figure 3.10: Hourly Overall Load for a Year on Distribution Network.....	42
Figure 3.11: Markov-Chain Based Battery Charging-Discharging Transition Diagram..	45
Figure 3.12: Markov-Chain Based Battery Charging-Discharging Transition Diagram..	46
Figure 3.13: Histogram of Power Transfer for 8760 Samples.....	52
Figure 3.14: Pareto Set of 100 Solutions	55
Figure 3.15: Reduced Pareto Optimal Set of Battery Size-Loss of Load Probability	56
Figure 3.16: Reduced Pareto Optimal Set of Battery Size-Availability	57
Figure 4.1: Algorithm for Monte Carlo Simulation (MCS).....	61
Figure 5.1: IEEE 33 bus distribution system	64
Figure 5.2: Proposed Algorithm for Restoring Loads – the Ultimate Microgrid	67
Figure 5.3: Optimal Reconfigured Microgrid Network for Case 3	78
Figure 5.4: Optimal Reconfigured Network for Case 4.....	80

LIST OF ABBREVIATIONS

MG	:	Microgrid
IBGA	:	Improved Binary Genetic Algorithm
DG	:	Distributed Generator
MCS	:	Monte Carlo Simulation
DN	:	Distribution Network
DSM	:	Demand Side Management
ENS	:	Energy Not Supplied
SAIFI	:	System Average Interruption Frequency Index
SAIDI	:	System Average Interruption Duration Index
PV	:	Photovoltaic
PC	:	Pick Clipping / Priority Customer
RE	:	Renewable Energy
SOC	:	State of Charge
GA	:	Genetic Algorithm
RES	:	Renewable Energy Sources
AI	:	Artificial Intelligent / Artificial Intelligence

MES	:	Mean Square Error
STC	:	Standard Test Condition
NOCT	:	Normal Operating Cell Temperature
CB	:	Circuit Breaker
MT	:	Mission Time
MPP	:	Maximum Power Point
SD	:	Standard Deviation
LOLP	:	Loss of Load Probability
BP	:	Bus Point

|

ABSTRACT

Full Name : [Md. Ilius Hasan Pathan]
Thesis Title : [Intelligent Smart Restoration Technique for Microgrids]
Major Field : [Electrical Power]
Date of Degree : [December 2017]

The concept of the microgrid in the electrical distribution system is gaining tremendous interest in recent decades to the researchers, governments, and utilities due to its advantages over conventional distribution networks. Moreover, integration of renewable energy into microgrid results in global reduction of carbon footprint. However, the intermittency of solar photovoltaic (PV) and wind energy has made them a challenge in terms of integration and utilization on the distribution side. In this regard, hybridization in the microgrid, particularly including solar PV, wind energy, energy storage and small-scale diesel generator, is creating a great possibility for highly reliable and dispatchable energy system. Therefore, this thesis has proposed an algorithm based on an improved binary genetic algorithm (IBGA) for managing outages in a hybrid microgrid.

This algorithm also optimizes the output of diesel generator to be integrated into the network and finds optimal locations for connecting distributed generators (DGs) and appropriate demand side management (DSM) implementation. Four operational constraints, namely – radiality, priority list, bus voltage and branch power flow, are considered in the optimization. Three objective functions, energy not supplied (ENS), system average interruption frequency index (SAIFI), and system average interruption duration index (SAIDI), are converted to a single objective function format as a minimization problem. In order to maintain practicality, DGs and loads are modeled

stochastically and an intelligent priority list is proposed. The output of DGs, load values, and priority list are made ready before including them in the restoration algorithm. All simulations are conducted in MATLAB environment where MATPOWER6 software is linked with MATLAB to test power flow constraints. The proposed algorithm has been implemented on IEEE 33 bus distribution system and the obtained results validate the effectiveness of the proposed algorithm. |

ملخص الرسالة

الاسم الكامل: محمد إلياس حسن بتحان

عنوان الرسالة: التقنية الذكية للإرجاع الذكي للشبكات المصغرة

التخصص: الطاقة الكهربائية

تاريخ الدرجة العلمية: ديسمبر ٢٠١٧

إن مفهوم الميكروغريد (الشبكة المصغرة) في نظام التوزيع الكهربائي يكتسب اهتماماً هائلاً في العقود الأخيرة من قبل الباحثين والحكومات والشركات بسبب مزاياه على شبكات التوزيع التقليدية. علاوةً على ذلك، فإن دمج مصادر الطاقة المتجددة في الميكروغريد سيساهم في الحد من انبعاثات الكربون العالمية. ومع ذلك، فإن تقطع الطاقة الشمسية الكهروضوئية وطاقة الرياح يجعل منهما تحدياً من حيث الدمج والاستفادة من ناحية التوزيع. في هذا الصدد، فإن التهجين في الميكروغريد، بما في ذلك الطاقة الشمسية الكهروضوئية، و طاقة الرياح، وتخزين الطاقة، ومولدات الديزل الصغيرة، سيخلق إمكانيةً كبيرةً لنظام طاقةٍ موثوقٍ بها للغاية و قابلةٍ للتوزيع. لذلك، تقدم هذه الأطروحة خوارزميةً تقوم على الخوارزمية الجينية الثنائية المعدلة (IBGA) لإدارة انقطاعات الكهرباء في الميكروغريد الهجين وهي طريقة تحسينٍ أمثلٍ بإعادة التشكيل طوبولوجياً.

تعمل هذه الخوارزمية على تحسين إنتاج مولدات الديزل ليتم دمجها في الشبكة وتحديد المواقع المثلى لربط المولدات الموزعة (DG) وتنفيذٍ مناسبٍ لإدارة الطلب على الطاقة (DSM). يتم النظر في أربعة قيود تشغيلية في خوارزمية التحسين الأمثل، وهي: الشعاعية، و قائمة الأولوية، والجهد الكهربائي، وتدفق الطاقة الفرعية. يتم تحويل ثلاث دوالٍ هدفيةٍ و هي: الطاقة غير المزودة (ENS)، و مؤشر معدل تكرار انقطاع النظام (SAIFI)، و مؤشر معدل مدة انقطاع النظام (SAIDI) إلى دالة هدفٍ واحدةٍ لتشكل معادلة تصغيرٍ أمثل. من أجل الحفاظ على التطبيق العملي، تم نمذجة المولدات الموزعة و الأحمال عشوائياً واقتراح قائمة أولوية ذكية. مخرجات المولدات الموزعة، وقيم الأحمال، وقائمة الأولويات تجهز عن طريق إجراء محاكاة لمرحلة التخطيط قبل تضمينها في خوارزمية الإرجاع. يتم إجراء جميع عمليات المحاكاة في بيئة ماتلاب (MATLAB) حيث يُربط برنامج MATPOWER6 مع ماتلاب لاختبار قيود تدفق الطاقة. وقد تم تطبيق الخوارزمية المقترحة على نظام توزيع IEEE 33، والنتائج التي تم الحصول عليها تُؤكد فعالية الخوارزمية المقترحة.

CHAPTER 1

INTRODUCTION

1.1 Electric Microgrid

The demand of electric power is in a fast-increasing mode in recent decades has caused the power system more increasingly complex interconnected grid to transmit the power to the load side. This complex grid system has brought the challenges in the security issue and enforced to operate as more sustainable, reliable and controllable scheme of energy systems. Therefore, the governments and responsible power entities are seeking solutions in microgrids in the distribution area – the building blocks for the ultimate smart grid in future. The distribution network, essentially known as the microgrid, is a consortium of distributed generators; wind turbines, solar photovoltaic (PV) power, biomass, geothermal and other renewable sources and energy storage with conventional small-scale fossil fuel generators in the distribution area.

It also facilitates the power balancing capability function between demand and supply for the both – loads and utility, comprehended as a single entity [1]–[4]. The microgrid also allows the bidirectional power flow to and from the main grid through a communication for proper controlling and supplying more reliable power to the consumers [4]. One of the important features of the microgrid is to operate in two modes – grid connected or islanded mode in which automatic controlling and communication schemes enable to operate in an islanded mode in any unusual condition of the main grid by disconnecting from the utility

[3], [5]. This standalone mode operation increases the microgrid's power availability and reliability. In addition, the utility can monitor the loads from distance in microgrid system owing to its highly controlling and communication schemes. All the aforementioned features conceptualize the microgrids making it enough smart in power operation – the smart grid in a broader view.

1.2 Motivation

The main challenge of the power utility organizations is to supply sustainable and reliable power to the consumers. Therefore, the balancing between supply and demand must be gained at all the time to overcome this challenge that perceives the electricity as a fresh commodity. In the year 2002 in the US, the revenue of total retailer electricity was \$249 billion whereas the total estimated outage cost was \$79 billion in the same year that is equal to 31.7 % of the revenue [6]. An outage costs comparison is made between North America and Europe in reference [7].

There are some reasons which make today's conventional power grid less reliable – the manual communication between customers and utility during outage periods which causes delay in restoration of the system, utility's unavailability to detect the system's instability prior to going into outage condition and, lack of proper load prioritization with demand side management during outage periods and peak load condition. These problems can be solved with the use of microgrid in the distribution area. Since the advanced information technological infrastructure, advanced metering infrastructure (AMI) and automatic control scheme are implemented in the microgrid which provide prior fault information, enable load side management, remote monitoring and controlling and, self-healing automation rather than manual restoration. Furthermore, microgrid uses the renewable energy sources as

distributed generations which are green sources of energy and, as a result, the carbon footprint owing to fossil fuels emission is reduced. As in reality, the load demands can never be constant at all the times but the generation of dispatchable swing units can ramp up and down to balance the load demands which is the conventional power operational scheme.

In microgrids, some renewable distributed generators are integrated into the system to increase the reliability in case of any fault or unavailability of dispatchable units. But, uncontrollable and intermittent nature of most of the renewable energy sources, especially solar and wind energies, make them costly. Both the sources depend on the time of the day, seasons and unpredictable weather conditions. Sometimes they generate more than the demand that is required at that time and sometimes it is less which does not mean the lack of total solar and wind energies to meet the load demands – hence the storage system can overcome the unpredictability of solar and wind energy generation by storing energy at excess generation periods and meeting deficiency at less or no generation periods.

In some cases, outages may cause a larger amount of deviation between demand and supply. As a result, solar and wind energies with storage system cannot meet the demand integrating the interrupted supply system. In this case, peak clipping (PC) demand side management (DSM) and diesel generator can be integrated into the supply system to increase the reliability of the distribution systems. Also, the optimal priority list of the loads is an important measurement for shedding the loads in case of any necessity which can also improve the reliability of the distribution systems supplying more important loads rather to less important loads at the outage time.

In order to synchronize the generated power with load demands at all the time, parameters of the distributed generators (DGs), such as sizing and sitting, must be optimized for making effective and efficient smart grid. In this case, the system will be able to supply sustainable and reliable power to the customers at minimum cost. Moreover, in case of emergencies and outages, a strategic self-healing restoration technique must be incorporated in a most optimized way considering DSM implementation and optimized load priority list. The quest what motivates for this thesis is all the aforementioned optimization fleet.

1.3 Objectives

The objectives are summarized below:

- ❖ To model the energy storage system (DG) and renewable DGs – solar photovoltaic and wind turbine – and analyze the reliability impact of these DGs on power distribution system.
- ❖ To propose a dynamic and intelligent load priority list model for microgrid based on the effect of DSM programs, criticality of loads, load point reliability indices and cost of interruption of each load at different hours. Fuzzy decision-making technique is proposed to obtain the overall numeric priority value from different priority indicator parameters for each load.
- ❖ To develop a smart load restoring optimization technique using improved binary Genetic Algorithm (IBGA) for microgrid system based on type, size and location of DGs and, supply availability, stochastic load demand, dynamic priority list, and integration of DSM program at proper position(s).
- ❖ To analyze the reliability indices of the re-configured microgrid system.

1.4 Contribution of this Thesis

The contributions of this thesis are summarized below:

- ❖ Time series based forecasting equation is modified and fuzzy time series-Markov chain technique is used to forecast temperature, wind speed and solar radiation.
- ❖ This thesis has proposed a new state transition matrix where the fixed zeros of the diagonal entries are replaced by a quantitative probability keeping compatibility with the assumption of discrete state of charge (SOC) which is ignored in the literature.
- ❖ Multi-objective clustering and fuzzy decision making (FDM) techniques are proposed for properly sizing the storage system instead of using conventional way.
- ❖ Dynamic priority list model is developed to optimize numeric priority value for each load using intelligent technique and implemented in load shedding using proposed algorithm during load restoring optimization.
- ❖ To propose an algorithm for restoring maximum amount of loads after occurring fault in distribution networks based on improved binary Genetic Algorithm (IBGA).

1.5 Thesis Organization

Literature related to this thesis work is reviewed in chapter 2. This includes the pros and cons reviewing of integrating distributed generators (DGs) and demand side management (DSM) during network reconfiguration. Literature related to integrating the priority list

during network reconfiguration is also presented in this chapter. In chapter 3, forecasting technique and mathematical models of DGs are discussed. This chapter also includes the evaluation of DG models.

Chapter 4 summarizes the objective functions and constraints. A brief discussion about Genetic Algorithm is also presented in this chapter. Simulation results of network reconfiguration based on the proposed algorithm considering fault in IEEE 33 bus distribution system is presented in the fifth chapter. Finally, the last chapter includes the concluding paragraphs and proposes some possible future works.

|

CHAPTER 2

LITERATURE REVIEW

2.1 Impact of Distributed Generators on Distribution Networks

With the change of living style of people around distribution area in recent days due to using technologically developed equipment, the aspects of distribution networks are also being changed towards highly reliable power supply to the consumers, especially for the critical load consumers. The conventional power operational systems are becoming more sophisticated and interconnected grid system to transmit bulk amount power to the load center in several paths from distant plants to reduce generation costs. This power management scheme draws the disadvantages at the time of any outage owing to natural calamity or any other major accidents resulting disconnection of a large number of consumers [8] – hence the solution is interconnected microgrid system in the distribution area.

The microgrid is considered as an interconnected system that consists some micro power sources those can be the single type or varieties, with loads as a single entity where the PV panels and wind generators of capability mostly less than 500kW are the typical types of micro sources [9], [10]. Furthermore, environmental effects will be reduced owing to using renewable DGs in the distribution areas which will also increase the system's reliability [11]. In references [12]–[15], some studies were conducted on reliability indices based on distributed generators. In reference [16], the authors mainly focused the effect on price in the retail markets due to the integration of distributed generators.

In this case, it was shown that the power loss in the distribution network is reduced and voltage profile is improved owing to using DGs. The proposed observation was implemented in IEEE-33 bus distribution system using genetic algorithm (GA). Investigation on the integration of maximum allowable DG output in the distribution network for connecting the maximum load and reducing power losses with best network topology was done using modified GA where few locations for connecting DGs were considered [17].

Research is going on to improve the performance and reliability of the distribution networks using different intelligent optimization techniques. In this regard, DGs can play an important role. Researchers are especially concerned in improving voltage profile, reduction of power losses – active and reactive – increasing the loadability of the system, decreasing the line flows, and improving the reliability indices etc. by penetrating the DGs in the networks and optimizing the best topology to supply power to the customers. In this case, Genetic Algorithm (GA), Particle Swarm Optimization (PSO), multi-objective optimization of different types etc. were used in the literature [18]–[22]. Though most of the cases multi-objective optimization was considered that is the usual scenario for distribution network reconfiguration, sometimes single objective was also considered. The minimum number of switching operations and the maximum number of loads to be restored according to the load priority sequence after isolation the fault following the current, voltage and radial network topology constraints were investigated for balanced and unbalanced networks considering both cases – with and without DG connection [23]. The proposed method was tested in the IEEE-33 bus system and shown the significantly improved voltage profile when DGs were connected to the network. Authors in [24] conducted a survey on the IEEE-33 bus system

and Tai-Power system to reduce the power losses of the systems and achieve the better load balancing using Artificial Ant Colony (AAC) algorithm for two cases – with and without DGs in the topology. Results shown an improvement when DGs were connected to the topology. But still, the research of the impact of distributed generators on distribution networks is insufficient. It is because that most of the cases the authors didn't consider the type of DGs rather only taken a certain amount of power in one or more buses to evaluate the effect of DGs on distribution networks.

Although few papers evaluated the effects of DGs on distribution networks considering its types, especially for renewable energies (RE) – PV and wind types, they excluded the intermittent and uncontrollable nature of renewable energy taking only the deterministic values. But the PV and wind power are fully dependent on nature. Also, the loads in power system are volatile in nature that could be modeled probabilistically rather considering deterministic value which was ignored in the literature.

Distribution systems must be maintained in balanced way in case of load demand and available supply which can be achieved taking into account storage systems and back up diesel power units in the distribution networks (DN) since the load, PV and wind power all are volatile in nature and have no control over PV and wind power generation. Therefore, the effect of DGs on distribution systems must be evaluated considering all the aforementioned features at the same time – that is not done yet in the literature in accordance with author's knowledge. In this case, evaluated distribution systems including aforementioned features can be considered as a perfect microgrid. It can also be mentioned that both the controlling schemes – grid connected and islanded mode are possible to

implement in microgrid (MG) which will increase the reliability of the system – the ultimate target in near future.

2.2 Demand Side Management

The influence to the consumers to use the energy at the proper time and suitable amount by some specific kinds of planning, implementation, and evaluation was comprehended as demand side management (DSM) program [25]. DSM has an effect on load to match with the generation by proper shaping which results in a reduction of generation cost. In case of consumer's point of view, consumers can get benefits from the utility due to timely using energy that causes the reduction of price per kWh of them and more sustained power supply. Several research works were made in the past using DSM on the reliability of distribution systems [26]–[29]. Two ways demand side management was handled by four Spanish Universities and this DSM was accomplished using Physically-Based Load Models (PBLM) of loads [30]. In reference [31], quality control for customer's satisfaction maintaining demand side management was achieved by including diesel generator, solar PV, and energy storage in IEEE 13 bus system and converting it to islanded mode microgrid. The authors also implemented the technique in real time simulator, OPAL-RT simulator, and in microcontroller based system. Distribution networks were dispatched as a microgrid scheme by including demand side management and energy storage system in [32], and the effectiveness was tested in a real system that consists of buildings and roof-top PV system. Demand side management was focused to reduce the overall operational costs and the cost of customer's utility usage in [33]–[37] to make the distribution systems smart.

Some authors optimized the locations and size of the storage system of microgrid including two objectives – giving some incentive to the customers owing to shifting loads and

reduction of line loss. In addition, communication was included in the smart distribution system for exchanging information between the utility company and customers in participating demand management following dual objectives – price based and reward based. This method was implemented in IEEE 37 bus distribution system. However, in some cases, load shifting and peak clipping both were included in demand side management by including customer's participation in microgrid for a day ahead cost reduction operation planning through investigation of power loss and voltage deviation. The authors in reference [38] evaluated the impact of load shifting from one hour to other hours on the performance of power transmission to find the optimal DSM. This model was tested using IEEE 9 bus transmission system and 295 bus generic distribution networks. A technique for managing demand response in distribution systems was proposed making it flexible to three phase grid in [39]. Demand side management using electric vehicles based on extended optimal power flow was proposed to accumulate power from different non-dispatchable renewable energy sources [40]. The algorithm investigated that how to reduce the extra costs by not upgrading the existing distribution network in the UK taking power from electric vehicles. Domestic energy consumption was managed by shifting loads from peak hours to off-peak hours using storage media so that demand of customers becomes responsive according to the needs of the utility company. In this case, charging and discharging factors were considered for analyzing the cost of the system [41]. To evaluate the model, the authors chose a UK household load profile.

But there is still a lack in research on reliability combining multiple effects with the stochastic mode, like the inclusion of renewable (RE) DGs, diesel DGs, storage and DSM programs, as the renewable sources – PV power and wind energy, are full of uncontrollable

and probabilistic in nature. Few papers evaluated the microgrids considering multiple effects [42], [43] but no work is done yet according to author's knowledge including all types of DGs with DSM programs and in case of necessity, load shedding action implementation in accordance with priority sequence.

2.3 Placement and Sizing of DG for Reliability Improvement

The investigation was made for proper placement of DGs in case of reliability improvement of the distribution networks in references [44]–[49]. Mainly DGs placements and capacity were evaluated in these pieces of literature. Though they analyzed the DGs capacity, the reliability of the microgrids was extensively affected owing to the variability of PV and wind energies. Some of them considered the cost effect for the case of sizing of DG. Obviously, to overcome the output variability problem, whenever the storage system will be considered, cost of storage system must be considered at the same time for optimizing the parameters.

Ant Colony Optimization (ACO) technique was implemented to dispatch the generation of renewable energy sources (RES) with cost optimization excluding the storage systems to overcome the variability of output [50]. Reliability, cost of energy, and power loss were analyzed in reference [51] for sitting and sizing of different types of DGs using multi-objective optimization without considering the storage systems. Model for locating and sizing of the solar farm was developed using multi-objective Bee optimization (MBO) to minimize the costs and emission of generation considering solar radiation [52]. Though they found the clustered Pareto set of solutions and fuzzy best-compromised solution, they didn't consider the variability of solar output which will change its reliability. Without considering

the storage systems, Markov chain rules were implemented to dispatch the PV plant output for analyzing the reliability in real time distribution networks in Egypt [53].

Though in [54], Artificial Bee Colony (ABC) based multi-objective optimization was implemented to increase the reliability of distribution system considering both, DGs and battery, they didn't give emphasize on charging and discharging procedure of battery which may result in over-sizing and costs.

The references [55], [56] focused the summation of all the time intervals within a certain time period for reliability analyzing when the demand of load exists but the storage systems can't meet the load demands. This strategy will provide an expected amount of estimated time when the loads are not powered by the DG system, but it does not give the probability of meeting the load demands by the DG system. Authors in [57] investigated the reliability by reconfiguring the distribution networks but still, they didn't consider the kinds of DGs – like PV panel and wind turbine. To overcome the output variability, availability was analyzed using the battery sizing concept to compensate the unavailability of power sources to power the load demands [58], [59]. Because of following simple method for analyzing the reliability, over or under sizing may cause which will increase the system cost or may cause the large variations of system loads successively.

The investigation was conducted in offline mode for a year to find out the optimal size and locations of DGs from some specific locations to reduce ENS and power loss and achieved optimal network configuration for improving the reliability of the system using Non-dominated Sorting Genetic Algorithm (NSGA) where the constant load was considered [60]. A similar analysis was done but includes more reliability indices with load modeling using

GA and PSO techniques in [19]. Non-dominated Sorting Genetic Algorithm (NSGA-II) was used for simultaneously reconfiguring the distribution network with proper placement of not only DGs but also capacitor bank considering three objectives – power loss minimization, voltage profile improvement and minimizing current loadability of the topology [20]. The authors claimed that their proposed method can be implemented in both phases – planning and operations – examined their algorithm considering some outage cases of the capacitor and distributed generators.

Most of the authors included the minimization of power loss and improvement of voltage profile in their optimization fleet following operational constraints and finding optimal locations and size of DGs for optimal network configuration. In some cases, it was found in the literature to be evaluated the number of DGs and its locations either in IEEE-33 bus test system or IEEE-69 bus system or both using artificial intelligence keeping total penetration constant [21], [61], [62]. But still, lack in research owing to not to be included the renewable energies with the probabilistic model which is one of the important features of the future microgrids to make the distribution network (DN) environmentally green. Moreover, very few papers considered the storage system to overcome the problem due to including the intermittent and uncontrollable weather dependent PV and wind power in the analysis but excluded the sizing of the storage system at the same time which may lead oversizing or under sizing of it.

2.4 Network Reconfiguration Technique

In literature [63], a multi-objective heuristic technique based on branch exchange was applied for reconfiguring the distribution networks in planning phase without considering any fault in the system to minimize the power losses and maximum branch current

maintaining operational constraints. Although the technique provided Pareto Front of switching sequences, still lacks in including some features like DGs consideration, priority list maintaining etc. The distribution system was reconfigured after initiating single fault to minimize power losses as a single objective function using improved Genetic Algorithm (IGA) where the uniform crossover was made in the reproduction process and shown a better result than GA in reference [64]. In this regard, the fault was initiated using Monte Carlo Simulation (MCS) and implemented in IEEE-69 bus system where the radiality constraint was maintained opening the number of branches exactly equal to the number of tie lines. Network reconfiguration after any disturbance needs to be within shortest possible time whilst technical aspects are maintained.

The past work conducted in reference [65] focused to reduce the computational burden while tri-objectives optimization problem was formulated considering power losses, outage areas and switching operations to be minimized maintaining all technical aspects. In this regard, penalty strategy was hybridized with normal GA to reduce the search space and shown better result compared to GA. They claimed that their method is applicable for online operation and tested in IEEE-33 bus system but didn't mention the technical constraints and its ranges those were maintained. Also, the reference didn't follow any probabilistic load model that is very practical as the load in power system is fully volatile in nature and ignored the DSM programs for an emergency. The Strength Pareto Evolutionary Algorithm 2 (SPEA 2) was used to solve the bi-objective optimization problem considering total loads to be restored and time required for reconfiguring the network after occurring any single or multiple faults in [66]. They said that owing to using a sub-permutation technique in the SPEA 2 algorithm, search space was reduced and less time was required to terminate the

program whilst five technical constraints were followed and it was almost order of few minutes for a large practical system. They excluded the consideration of all the types of DGs and any DSM program to be implemented to the distribution system with any load shedding schedule following a specific way in case of necessity. Therefore, the inclusion of all these features in the algorithm will definitely increase the simulation time that may make the method unfeasible for online operation as they claimed. Also, the reference proposed the priority sequence will not be valid when two or more clients will be interrupted for their maximum allowed duration.

Genetic Algorithm was used to reconfigure the microgrid considering RE generations and storage system following a priority sequence after fault occurrence in [67]. Although the method was tested in Real Time Digital Simulator (RTDS) software which was real-time implementation and they claimed satisfactory results, they didn't stochastically model the load and RE generations which is weather dependent and volatile in nature. They chose deterministic value rather optimizing the sizes and locations of DGs and storage system and changed the structure of the topology to minimize the disconnected loads. The algorithm offered the islanded mode operation of the network which is a vital feature of microgrid but didn't take into account the DSM programs in case of necessity. In the past work [68], four objective functions were optimized simultaneously using Genetic Algorithm following priority sequence without any other extra features to reconfigure the distribution network after fault occurrence.

In the recent days, the technological development has changed the vision of the power clients to receive electricity from uninterrupted and highly reliable source for making a safe coherence between their life and the technologies that are using. This is because the utility

companies are also trying to supply electricity to their customers fulfilling the customer's satisfaction level. Also, the deregulated concept in the electricity market has increased the competition among the utility companies that results in an increase of awareness of the companies towards the reliable supply electricity to their customers. As a result, different artificial intelligent techniques are being used for both mode of operations – online or offline – to improve the distribution topology by reconfiguring and restoring the maximum number of loads after any fault. In this case, reducing the simulation burden, minimizing power losses and switching operations after reconfiguration, considering priority sequence, sizing, and locating of DGs are considered to be optimized following operational constraints which make the system multi-objectives and multi-constraints type of problem. The techniques those were included in the literature in optimizing these fleet of objectives were the binary PSO [69], NSGA [60], hybrid PSO and Tabu search [70], GA [21], [71]–[73], NSGA-II [74], Invasive Weed Optimization Algorithm [61], Harmony Search Algorithm (HSA) [22], Ant Colony Algorithm (ACA) [24], Evolutionary Programming (EP) [75], Combination of Fuzzy-Genetic Algorithm [76] and Improved Genetic Algorithm (IGA) [77] etc.

2.5 Restoration Priority Listing

A proficient power restoration technique has become a necessity in recent days to improve the reliability of distribution networks for synchronizing the society's need in case of reducing the interruption costs and supplying secured and sustainable power to them. One of the aspects of the efficient restoration process is the prioritizing the load importance from the critical label to normal loads, even for the loads, those can be curtailed by paying penalty whenever an outage occurs. Importance of the loads is expressed as a numerical

value by assigning their weights and ranked according to their weighted values what are considered as the input of power restoration process.

But, the importance of load is dynamic in nature (i.e. time-dependent) that will be updated with time. For instance, the feeder that connects some institutions must get higher priority during the daytime whereas at nighttime the scenario will be reversed. This importance depends on several factors – the number of connected customers; can be represented by SAIFI and SAIDI, the amount of energy consumed by the loads which can be represented by ENS and cost of interruptions. Besides, this load prioritizing procedure considers the criticality of loads and demand side management (DSM) programs by positively or negatively adding some weights with original numerical importance and similarly some other factors.

The customers who are defined as priority customers (PCs) – include hospitals, fire services, information center, banks, security departments, large factories and so on, cannot be alleviated their loss at the time of power failure. Therefore, it is necessary to restore those customers as shortest time as possible. These customers are commonly connected to the microgrid systems. In case of criticality, priority is given regardless the amount of power consumed or the number of customers is connected. For instance, a hospital will get more preference to be restored with power connection within quickest possible time than any other loads either consuming a large amount of power or a large number of customers are connected. Obviously, priority classification will consider the importance of that corresponding load; definitely the information center will be more preferred than the banks although both are priority type customers. Again, the governmental offices will get more

preference during weekdays than the weekend or office hours will be considered the more preferred time to restore immediately than when it is not the office hours (i.e. nighttime).

Currently, the restoration process is made based on operator judgment prioritization which is not dynamic prioritization process and the resulted decisions may have a negative impact on the distribution networks in case of reliability or may cause a big loss. Some past works were conducted considering only simple importance level. Multi-objective service restoration technique was proposed considering priority customers (PCs) which was tested in small real-time Brazilian distribution system [78]. Artificial Neural Networks (ANN) based restoration problem was proposed, tested, and examined on a 162-bus system [79]. Although its real-time implementation made the proposed approach significant, the method still has a lack of precision owing to not implementing the priority list in it.

In reference [80]–[82], all the priority listed consumers were considered as the same level of important loads and put a single higher priority group for differentiating them from others where criticality was neglected for any of the loads. Risk priority based transformer replacement or repairing was conducted in reference [83] where only a single type of risk – number of customers out of service – was considered for the restoration process. In addition, multi-priority levels were considered for priority listing based restoration process in [84], [85]. Arguably the restoration process considering priority list was better than without priority list; still, it has lack of being fully precise and dynamical priority list.

Therefore, most of the aforementioned priority listing based restoration algorithm implemented the multi-objective evolutionary technique for making it a self-healing restoration process. In this case, one of the objectives was the priority customer listing

which lacked its precision due to less reflection of dynamical behavior. In this work, a priority listing approach is proposed including several levels of importance which is more than three with demand side management programs and level of criticality.

Moreover, time of the power consumption is considered in several categories – weekdays, weekend, office hours, off-period office hours, vacations for the institutional loads and seasonal effects, to make the list full of dynamic using one-hour time frame. In this case, the fuzzy compromised approach is implemented to assign a numerical membership value for each load considering four objectives – SAIFI, SAIDI, ENS and hourly cost of interruptions for a year mission time.

Although the past literature focused to increase the reliability of distribution networks through the implementation of different artificial intelligent (AI) techniques in optimizing the different objective functions, – such as sizing and siting of DGs including renewable energies, load shedding schedule, reconfiguring topological structure, minimizing simulation time, switching operations, SAIFI, SAIDI, ENS, costs and power losses etc. – still, there is a lack of research. Because, according to the author’s knowledge, no previous work evaluated the combined effect of at least the crucial objectives so that the DN can be considered as a perfect microgrid – the smart grid in a broader view.

It is already mentioned that the distribution network reconfiguration is a multi-objective and multi-constraint optimization problem. Therefore, this work has been formulated as a tri-objectives optimization problem in scalar form and Improved Binary Genetic Algorithm (IBGA) is used to optimize this problem. The work has considered four types of DGs – PV, wind turbine, storage system, and diesel generator – to be connected with the reconfigured

topology while the diesel DG is considered to be connected with the network in case of unavailability of total supply. The peak clipping (PC) DSM schedule and priority sequence have been included in this work where the priority list problem is formulated using intelligent technique considering five factors – SAIFI, SAIDI, ENS, interruption costs and DSM effect at each load point. In the final stage, one or more loads are shedded in needs according to the hourly priority list while all the operational constraints are fulfilled. Loads are modeled stochastically considering its volatile nature using standard deviation and historical mean values. Solar radiation, wind speed, and temperature are forecasted using Fuzzy Time Series-Markov Chain model based on historical value while a one-hour resolution is taken over one-year simulation period. Then the PV power is calculated using De Soto's 5-Parameter model [86] whereas the wind power is calculated using simple wind power model [44]. Moreover, the storage system is sized intelligently depending on how much percent of total load will be supplied using the solar system and wind turbine for ensuring a specific level of reliability (i.e. 0.99 or 0.999 ...).

Though the full capacity supply is considered for RE DGs, the diesel generator output is optimized in between the minimum and maximum capacity. For the case of the storage system, if the sum of total initial lost units during the considered outage period is less than the size of the storage, then the amount of storage output will be supplied at each hour to the network which is equal to the total lost load for that corresponding hour. Meanwhile, if the sum of total initial lost units during the considered outage period is more than the size of the storage, then the power from the storage will be supplied to the network at each hour during the outage period according to the hourly total post-fault lost load.

Finally, locations are also optimized for all DGs and DSM implementation. So far the author's knowledge, no past works have taken into account all the features together those are considered in this research to reconfigure the distribution networks to make it perfect microgrid – the ultimate smart grid in future.

CHAPTER 3

SYSTEM MODELING AND MODEL EVOLUTION

3.1 Forecasting Technique Modeling

Storage-based PV-Wind power sources will be more dispatchable for improved reliability in accordance with increasing the accuracy of forecasting the data, e.g., temperature data, solar radiation data, wind speed and load data. To achieve this goal, researchers are interested in the fuzzy time series technique for time series data rather than using the conventional technique for forecasting precisely that was first proposed by Song and Chissom [87]. In this case, the fuzzy logic theory is implemented in time series data known as fuzzy time series for forecasting a wide range of data categories more accurately as a linguistic value. In reference [88], authors have implemented the first order fuzzy time series to predict the enrollments of the University of Alabama, USA, whereas [89] predicts the temperature and Taiwan Future Exchanges (TAIFEX) using the same method and shows the method's accuracy. The same method on a higher level is used to forecast the temperature and Taiwan Future Exchanges in [90].

On the other hand, fuzzy time series is combined with the Markov chain model to forecast the data to increase its feasibility and accuracy in references [91]–[93]. Their primary focus was to forecast the temperature. But reference [94] utilizes a first order fuzzy time series-Markov chain to forecast the exchange rate between Taiwan and US Dollars, where the authors have compared and shown the lowest error (MAPE is 1.4042%) of this method.

Also, it is a free data pattern forecasting technique that is necessary for other forecasting techniques, i.e., Weibull, Ryleigh, exponential distributions, etc.

Because of the wide usability and accuracy of the proposed modified fuzzy time series-Markov chain-based forecasting technique, temperature, wind speed and solar radiation are predicted using this technique for reliability improvement analysis. A brief theoretical overview of this forecasting technique is discussed below.

3.1.1 Fuzzy Time Series-Markov Chain Model

Let $U(t)$ ($t = \dots, 0, 1, 2, 3, \dots$) be a universe of discourse which is a subset of real number R . Assume that the universe of discourse $U(t)$ defines $g_i(t)$ ($i = 1, 2, \dots$) and $G(t)$ consists of $g_i(t)$ ($i = 1, 2, \dots$). Then $G(t)$ is known as a fuzzy time series of $U(t)$ ($t = \dots, 0, 1, 2, 3, \dots$). In this case, $G(t) = G(t - 1) \circ R(t, t - 1)$, where $R(t, t - 1)$ is the fuzzy relationship and \circ is known as the max-min composition operator; then $G(t)$ is caused by $G(t - 1)$ and it is written as $G(t - 1) \rightarrow G(t)$, where $G(t - 1)$ & $G(t)$ are the fuzzy sets.

If the data are time-invariant as this work has dealt with, in this case, the relationship can be written as: $G(t) = G(t - 1)$. If time series data $G(t)$ is represented by B_i and $G(t - 1)$ is represented by B_j where k th data is included in the fuzzy relationship group and B_j and $(k + 1)$ th are included in B_i , then the fuzzy logical relationship within the universe of discourse can be written as " $B_j \rightarrow B_i$ ". In case of these two fuzzy logical relationship groups, B_j is considered the current state of the Markov chain transition diagram and B_i is the next state of the Markov chain transition diagram, where $i, j = 1, 2, 3, \dots, n$. According to the fuzzy relationship, if a state B_3 makes transitions to the other states within the

universe of discourse, like $B_3 \rightarrow B_3, B_3 \rightarrow B_4, B_3 \rightarrow B_5, \dots$ then it can be written as $B_3 \rightarrow B_3, B_4, B_5, \dots$ for the data are included within the groups.

Let us now explain how we can define the universe of discourse and fuzzy group of intervals for all the historical data within the universe. If D_{max} and D_{min} are the maximum and minimum values for specific historical data respectively, then the universal discourse for this historical data type can be defined as $[(D_{min} - D_1), (D_{max} + D_2)]$, where D_1 and D_2 are small positive values including zero but depending on the historical data type.

Now we can partition the universal discourse, U, into several equal intervals which actually represent the fuzzy logical groups with the maximum and minimum limits of each group. In this case, it can be written as $k = [(D_{max} + D_2) - (D_{min} - D_1)]/N$, where N is the number of intervals. Therefore, the partitioned intervals for the universe are obtained as:

$$m_1 = [(D_{min} - D_1), (D_{min} - D_1 + k)],$$

$$m_2 = [(D_{min} - D_1 + k), (D_{min} - D_1 + 2k)],$$

.....

$$m_N = [(D_{min} - D_1 + (N - 1)k), (D_{max} + D_2)].$$

As this work has considered a one-step first-order fuzzy time series-Markov chain model, therefore, fuzzy logical relationship groups can be written in terms of fuzzy intervals for fuzzification as:

$$B_1 \equiv m_1, B_2 \equiv m_2, \dots, B_N \equiv m_N.$$

Let a dataset have the “Z” number of data points collected considering a fixed resolution time period within a period of discourse. If “ n_1 ” numbers of data points at different time positions among “Z” data points are included in fuzzy logical interval group B_i state, all the “ n_1 ” data points transit to the next time positions from their current time positions.

The data points of the next time positions are included in three fuzzy logical group states, e.g., $B_{(i+2)}$, B_i & $B_{(i+3)}$ among all fuzzy logical group states (B_N) and “ n_2 ” numbers of the next time position’s data points among “ n_1 ” data points of the next time positions are included in $B_{(i+2)}$. Similarly, “ n_3 ” and “ n_4 ” data points of the next time positions are included in B_i and $B_{(i+3)}$ logical group states respectively, where $n_1 = n_2 + n_3 + n_4$. Then the transition probability from fuzzy logical state B_i to fuzzy logical state $B_{(i+2)}$ in a Markov chain logical state transition diagram is $P_{i,(i+2)} = n_2/n_1$. Similarly, the other two transition probabilities can be written as $P_{i,i} = n_3/n_1$ and $P_{i,(i+3)} = n_4/n_1$ since the total number of transitions from state B_i are “ n_1 ”. In the case of transiting from B_i state to other states, the Markov chain logical state transition diagram is shown in figure 3.1.

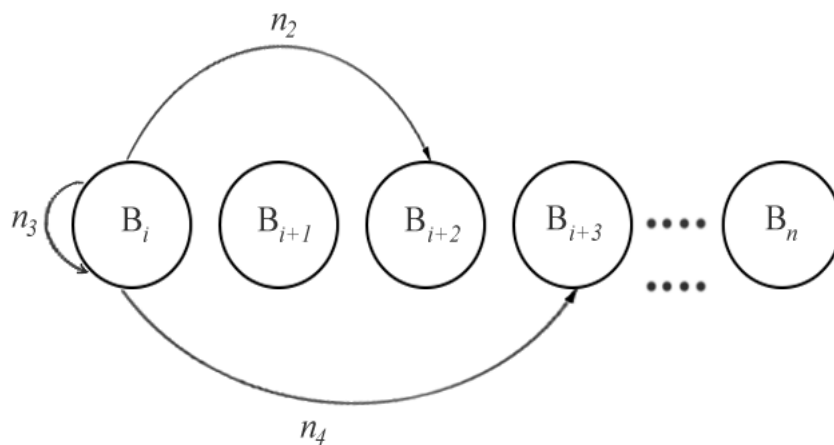


Figure 3.1: Fuzzy Time Series-Markov Chain State Transition Diagram

Therefore, the transition probabilities from state B_i to all other logical states are zero (i.e., $N - 3$ states have zero transition probabilities). The transitions from other states in figure 3.1 will occur accordingly. Now the state transition matrix can be represented for the whole system of fuzzy time series-Markov chain state transition diagram thusly: If the total number of transitions from i^{th} state to all other states are T_i and individual state transitions from i^{th} state to j^{th} state are $T_{i,j}$ and $i, j = 1, 2, 3, \dots$, then the fuzzy logical Markov chain transition probability matrix can be written as:

$$P = \begin{bmatrix} P_{11} & P_{12} & P_{13} & \dots & P_{1N} \\ P_{21} & P_{22} & P_{23} & \dots & P_{2N} \\ \dots & \dots & \dots & \dots & \dots \\ \dots & \dots & \dots & \dots & \dots \\ P_{N1} & P_{N2} & P_{N3} & \dots & P_{NN} \end{bmatrix} \quad (3.1)$$

where

$$P_{ij} = \frac{T_{ij}}{T_i}, \quad i, j = 1, 2, 3, \dots, N$$

Data are forecasted using this technique based on historical data in two steps.

Step 1: If time series data $G(t - 1)$ is included in logical state B_i and there is no transition from this state (It is only possible for the last state but not strictly always) to any other state, then it can be represented as: $G(t - 1) \equiv B_i \rightarrow \emptyset$, an empty state. In this case, forecasting of data for the next time position is defined as:

$$G(t) = h_i, \quad i = 1, 2, \dots, N \quad (3.2)$$

where

h_i is the mid-point of fuzzy logical interval group B_i .

Step 2: If time series data $G(t - 1)$ is included in logical state B_i and makes the transition, then it can be represented as: $G(t - 1) \equiv B_i$. In this case, two cases are considered and the row vector of the fuzzy logical Markov chain transition probability matrix, $[P_{i1} \ P_{i2} \ P_{i3} \ \dots \dots P_{iN}]$, is used to forecast the next time position data $G(t)$.

Case 1: If the transition occurs from fuzzy logical interval group B_i as a one-to-one condition (e.g., $B_i \rightarrow B_j$ with $P_{ij} = 1$ and $P_{ir} = 0$ for $j \neq r$, as the sum of each row of the probability matrix is always unity), then the forecasting of data of the next time position is defined as:

$$G(t) = h_j P_{ij} = h_j \quad (3.3)$$

where

h_j is the mid-point of fuzzy logical interval group B_j .

Case 2: If the transitions occur from fuzzy logical interval group B_i as a one-to-many condition (e.g., $B_i \rightarrow B_1, B_2, \dots, B_N$, meaning that at least two states exist among “N” states and $i = 1, 2, \dots, N$), then the forecasting of data for the next time position is defined according to the proposed modified equation as:

$$G(t) = h_1 P_{i1} + h_2 P_{i2} + \dots + h_{i-1} P_{i(i-1)} + \left(\frac{U(t-1) + U(t)}{2} \right) P_{ii} + h_{i+1} P_{i(i+1)} + \dots + h_N P_{iN} \quad (3.4)$$

where

h_1, h_2, \dots, h_N are the mid-points of fuzzy logical interval groups B_1, B_2, \dots, B_N .

In this case, this equation is modified to use the diagonal element of the fuzzy logical Markov chain transition probability matrix by replacing h_i with the average of the historical

data of the current time position and the next time position instead of using only the historical data of the current time position. It thus reflects a more accurate prediction, as we have considered each fuzzy logical interval group as a state instead of considering each time position data as a state.

Since there may occur some transitions between two-time positions data of different values, both the time positions data are included in same fuzzy logical interval group, which will translate transition in the same state. The example in table 3.1 will clarify the forecasting process.

Table 3.1: Sample Historical Values & Fuzzification

Time	Time Series Data & Fuzzification	Universal Discourse & Fuzzy Groups
1	5 (B1)	$D1=1, D2=1$ $U = [(5-1) (15+1)] = [4 \ 16]$ $k = (16-4)/(N=6) = 2;$ $m1 = [4 \ 6]$ $m2 = [6 \ 8]$ $m3 = [8 \ 10]$ $m4 = [10 \ 12]$ $m5 = [12 \ 14]$ $m6 = [14 \ 16]$
2	6 (B1)	
3	6 (B1)	
4	7 (B2)	
5	9 (B3)	
6	12 (B4)	
7	6 (B1)	
8	6 (B1)	
9	14 (B5)	
10	15 (B6)	

According to the example in table 3.1, the fuzzy logical relationship for the first state B_1 is $B_1 \rightarrow B_1, B_1, B_1, B_2, B_5$. Now, if we want to forecast at time 2, then it will be

$$G(2) = \left(\frac{5+6}{2}\right) * \frac{3}{5} + 7 * \frac{1}{5} + 0 + 0 + 13 * \frac{1}{5} = 7.3$$

where

the total number of transitions from state one is five.

3.1.2 Implementation of Fuzzy Time Series-Markov Chain Model

For forecasting the temperature, solar radiation and wind speed, hourly historical data are collected for 365 days. In this case, length of all data categories was the same, as one of the objectives of this study is to discover the charging-discharging process of the battery. The right histogram in figure 3.2 approximates the histogram of the forecasted temperature of 365 days, and the historical temperature is shown in the left side in figure 3.2, with mean square error (MSE) 169.37% using the proposed technique, whereas the other methods (i.e., Weibull, Ryleigh, exponential distributions) show the MSE at more than 1100%.

Though the temperature has a seasonal effect, this study has considered the seasonal effect only for predicting the solar radiation where four seasons are considered consecutively starting from January 1. After predicting the radiation of all the seasons, it is combined to make a complete year (365 days) of solar radiation data, where the algorithms are fitted to make the unity probability for predicting the radiation at nighttime (13 hours) always equal zero, which is the practical scenario.

The left two figures in figure 3.3 and figure 3.4 show the histograms of historical solar radiation data for season 1 and the whole year respectively, whereas the right ones in figure 3.3 and figure 3.4 approximate them respectively and are almost identical to the historical data.

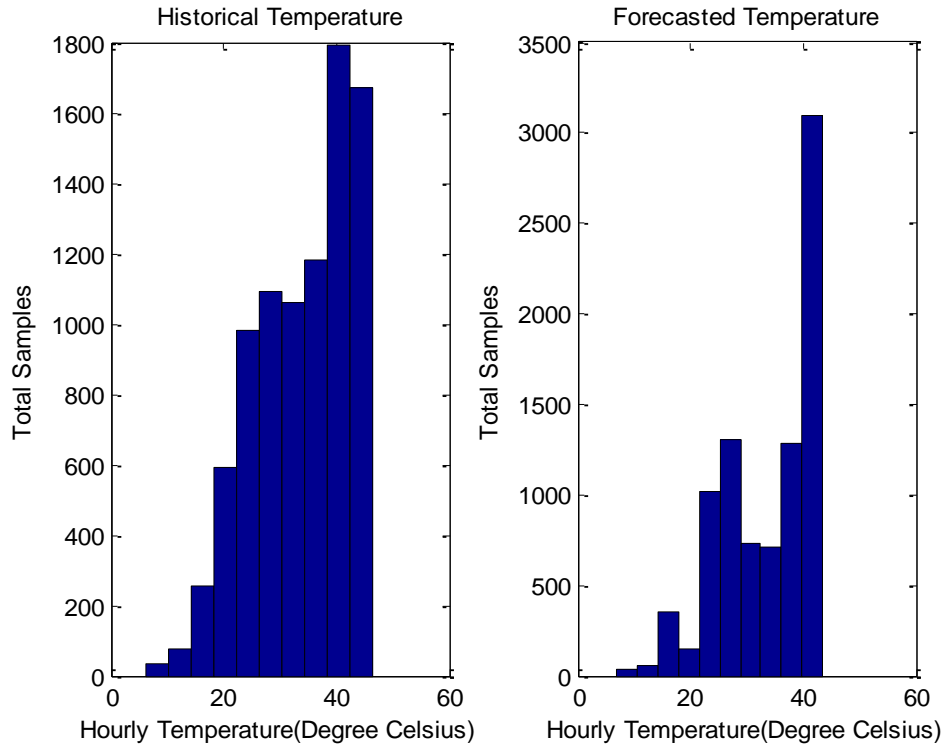


Figure 3.2: Histogram of Hourly Daytime & Nighttime Temperature of One Year

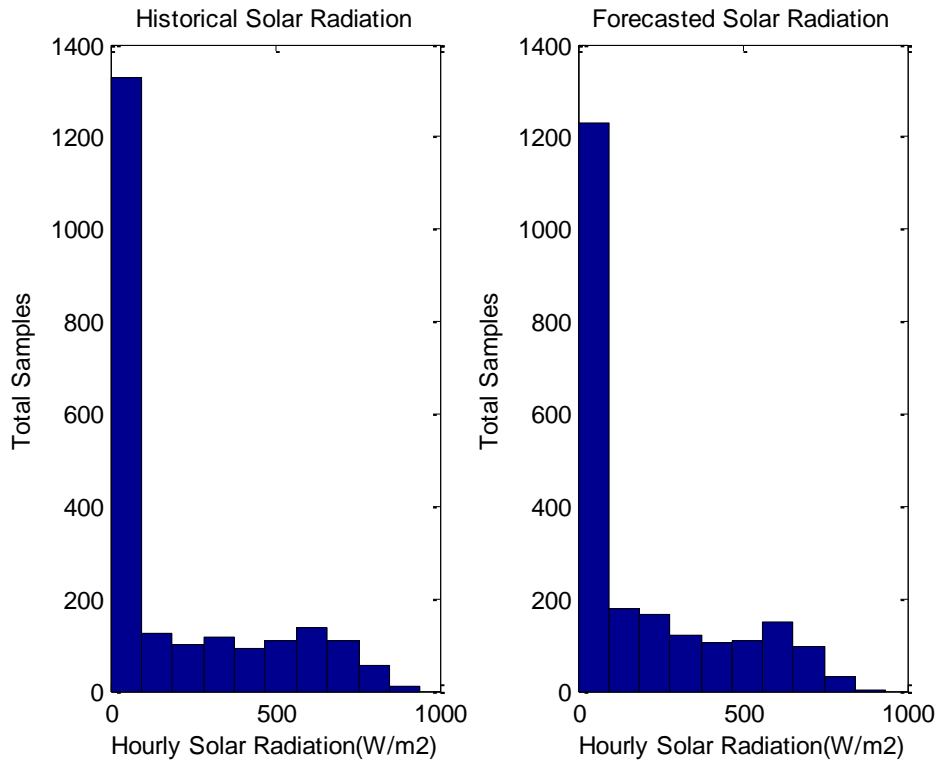


Figure 3.3: Histogram of Hourly Daytime & Nighttime Radiation of 1st Season (91 Days)

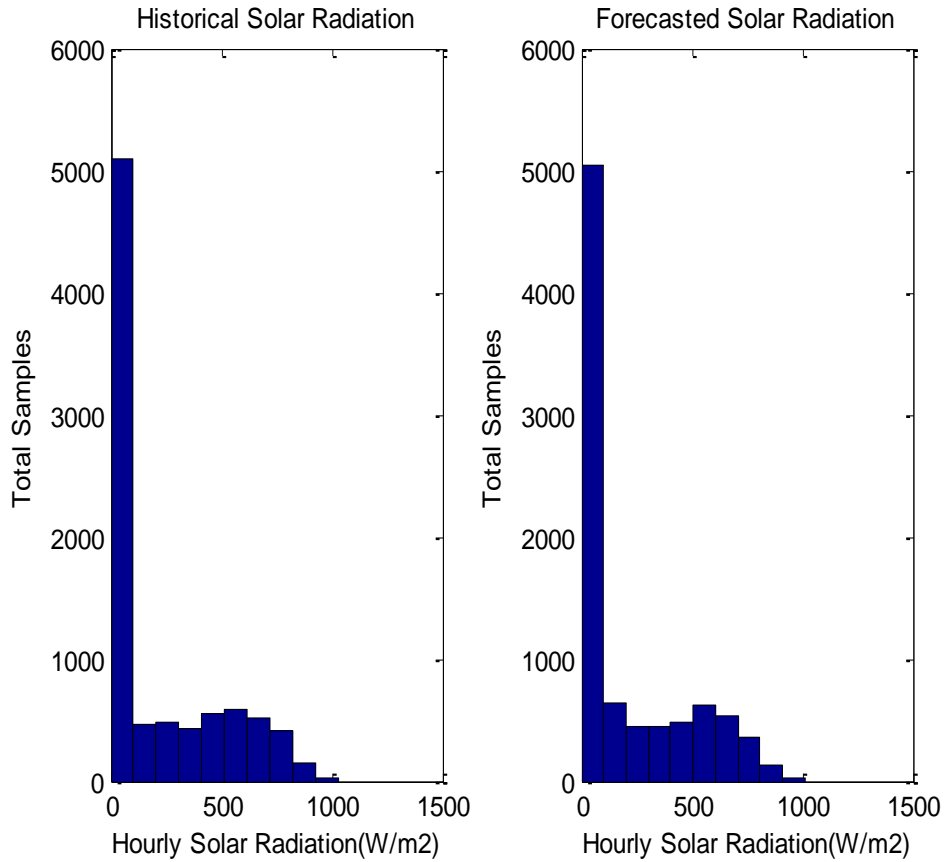


Figure 3.4: Histogram of Hourly Daytime & Nighttime Radiation of One Year

The left histogram in figure 3.5 shows the actual wind speed, whereas the histogram of the forecasted wind speed is shown in the right.

Since the fuzzy time series-Markov chain technique is a free data pattern forecasting technique, the histogram on the right side in figure 3.5 approximates an almost identical histogram on the left side that is the histogram of historical wind speed data. As a result, error due to forecasting using this technique is lower than the error due to using the other forecasting techniques (i.e., Ryleigh and exponential distributions, and even Weibull distribution).

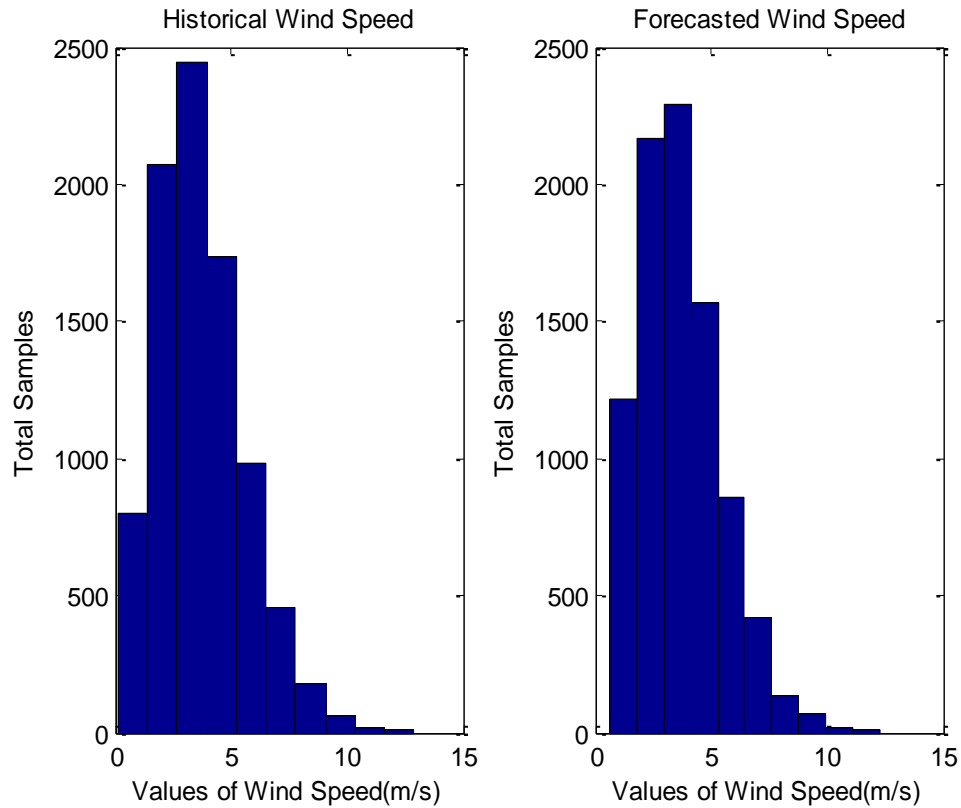


Figure 3.5: Histogram of Hourly Wind Speed of One Year

3.2 Photovoltaic (PV) DG Model

We know that the PV power depends not only on solar radiation and PV cell characteristics but also on the temperature that makes hot cells, which results in a reduction of PV power generation from same amount of radiation that generates PV power from cool cells. Temperature also reduces the efficiency of PV panels. In the literature, it is mentioned that the voltage of a PV panel is reduced typically by 0.35%-0.5% for each degree Celsius of temperature increase [95].

As the effect of changing the temperature on currents is very low, it can be assumed that PV power is reduced typically by 0.35%-0.5% due to increasing each degree Celsius of temperature. Effect of temperature on solar PV power generation is shown in reference [96], where it is claimed that performance of solar PV cells is better on cold and sunny days than

on sunny and hot days. Therefore, to make an effective microgrid system, temperature effect is effectively included in the reliability analysis of the distribution network (DN) through extracting PV power considering De Soto's 5-Parameter model [86], which was not taken into account in past works for reliability analysis of the DN. In this case, the manufacturers provided data, and fuzzy time series-Markov chain-based forecasted solar radiation and temperature are used. This model considers the effect of a hot or cold sunny day, including the PV cell temperature effect, to extract PV power under different ambient conditions. The solar PV model is characterized using five parameters proposed by De Soto, whose equivalent circuit is shown in below:

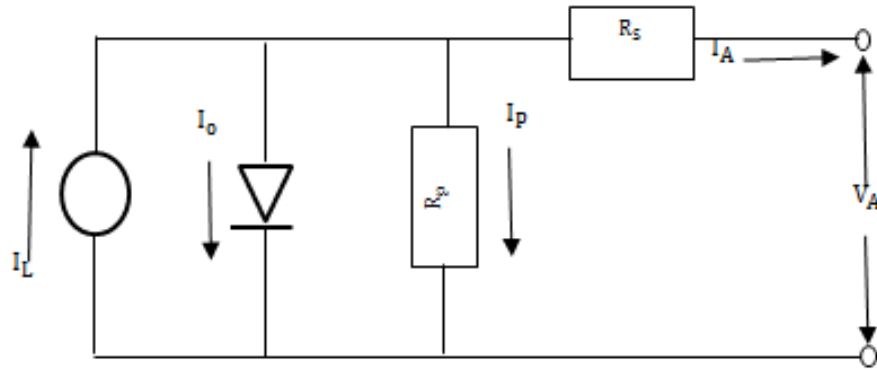


Figure 3.6: 5-Parameter Model Equivalent Circuit

The voltage-current relation of this model is given by equation (3.5):

$$I_A = I_L - I_o \left[e^{\frac{(V_A + I_A R_s)}{a}} - 1 \right] - \frac{V_A + I_A R_s}{R_p} \quad (3.5)$$

where

I_o is the reverse saturation current for the diode, I_L is light current, R_p is the shunt resistance, R_s is the series resistance of the Solar photovoltaic (PV) model, and a is ideality factor. After obtaining the five parameters (I_L, I_o, a, R_s, R_p), normally under standard test

conditions (STC), I-V characteristic curve and P-V characteristic curve can then be obtained. To obtain these two curves at other radiations and temperatures, it is necessary to calculate the parameters at the corresponding ambient conditions that relate to the changing of STC condition, which are expressed by the equations (3.6)-(3.11) [97]:

$$I_L = \left(\frac{G}{G_0}\right) [I_{L0} + \alpha_{I,sc}(T_c - T_{c0})] \quad (3.6)$$

$$I_o = I_{o0} \left(\frac{T_c}{T_{c0}}\right)^3 e^{\left[\frac{E_{g0}}{kT_{c0}} - \frac{E_g}{kT_c}\right]} \quad (3.7)$$

$$E_g = 1.17 - 4.73 \times 10^{-4} \left(\frac{T_c^2}{T_c + 636}\right) \quad (3.8)$$

$$\frac{R_p}{R_{p0}} = \frac{G_0}{G} \quad (3.9)$$

$$R_s = R_{s0} \quad (3.10)$$

$$\frac{a}{a_0} = \frac{T_c}{T_{c0}} \quad (3.11)$$

where

R_{p0} & R_{s0} are the shunt and series resistances of the solar PV model under STC successively, G_0 is the total solar irradiance under STC, G is the total solar irradiance under other conditions, $\alpha_{I,sc}$ is temperature coefficient for the short circuit current, I_{L0} is light current under STC, I_{sc0} is the short circuit current under STC, I_{o0} is the reverse saturation current for the diode under STC, E_{g0} is band gap energy of the material under STC, E_g is band gap energy of the material under other conditions, T_{c0} is the cell temperature under STC and T_c is the cell temperature under other conditions.

Information provided by the manufacturers is used with equations (3.12)-(3.18) to calculate all five parameters under STC.

$$0 = I_{L0} - I_{o0} \left[e^{\frac{V_{oc0}}{a_0}} - 1 \right] - \frac{V_{oc0}}{R_{p0}} \quad (3.12)$$

$$I_{sc0} = I_{L0} - I_{o0} \left[e^{\frac{I_{sc0}R_{s0}}{a_0}} - 1 \right] - \frac{I_{sc0}R_{s0}}{R_{p0}} \quad (3.13)$$

$$I_{mp0} = I_{L0} - I_{o0} \left[e^{\frac{(V_{mp0}+I_{mp0}R_{s0})}{a_0}} - 1 \right] - \frac{V_{mp0}+I_{mp0}R_{s0}}{R_{p0}} \quad (3.14)$$

$$\frac{I_{mp0}}{V_{mp0}} = \frac{\frac{I_{o0}}{a_0} e^{\frac{(V_{mp0}+I_{mp0}R_{s0})}{a_0}} + \frac{1}{R_{p0}}}{1 + \frac{I_{o0}R_{s0}}{a_0} e^{\frac{(V_{mp0}+I_{mp0}R_{s0})}{a_0}} + \frac{R_{s0}}{R_{p0}}} \quad (3.15)$$

$$\beta_T = \frac{\partial V_{oc}}{\partial T} = \frac{V_{oc} - V_{oc0}}{T_c - T_{c0}} \quad (3.16)$$

$$V_{oc} = V_{oc0} + \beta_T (T_c - T_{c0}) \quad (3.17)$$

$$0 = I_L - I_o \left[e^{\frac{V_{oc}}{a}} - 1 \right] - \frac{V_{oc}}{R_p} \quad (3.18)$$

where

I_{mp0} and V_{mp0} are the maximum power point current and voltage under STC respectively.

β_T is the temperature coefficient of the open circuit voltage, V_{oc} . The temperature range for equation (3.16) is taken between $T_c = T_{c0} - 17$ and $T_c = T_{c0} + 25$. Equations (3.19) and (3.20) are used to obtain the maximum power point (MPP) current and voltage under any ambient condition, whereas equation (3.21) gives the cell temperature based on normal operating cell temperature (NOCT), ambient temperature, T_{amb} , and irradiance level.

$$I_{mp} = I_L - I_o \left[e^{\frac{(V_{mp} + I_{mp}R_s)}{a}} - 1 \right] - \frac{V_{mp} + I_{mp}R_s}{R_p} \quad (3.19)$$

$$\frac{I_{mp}}{V_{mp}} = \frac{\frac{I_o}{a} e^{\frac{(V_{mp} + I_{mp}R_s)}{a}} + \frac{1}{R_p}}{1 + \frac{I_o R_s}{a} e^{\frac{(V_{mp} + I_{mp}R_s)}{a}} + \frac{R_s}{R_p}} \quad (3.20)$$

$$T_c = T_{amb} + G \left(\frac{NOCT - 20}{0.8} \right) \quad (3.21)$$

After obtaining the forecasted temperature and solar radiation data, the 5-parameter model is used to calculate the PV output power for a specific PV panel model. In this case, the specification of this panel is provided by the manufacturer. To characterize the solar DG model, Canadian Solar Max Power CS6X-320P solar panel has been considered in this study. A comparison of 5-parameter model output with manufacturer's specified output at two operating conditions – SRC and NOCT – is shown in table 3.2.

Table 3.2: 5-Parameter Model Output and CS6X-320P Datasheet Specification [98]

Operating Point	Parameters	320P Datasheet	Model
SRC 1000 W/m ² 25°C	P _{max} (W)	320	318.97
	V _{mpp} (V)	36.8	36.79
	I _{mpp} (A)	8.69	8.67
	V _{OC} (V)	45.3	45.33
	I _{SC} (A)	9.26	9.27
NOCT 800 W/m ² 47°C	P _{max} (W)	232	234.91
	V _{mpp} (V)	33.6	33.80
	I _{mpp} (A)	6.91	6.95
	V _{OC} (V)	41.6	42.24
	I _{SC} (A)	7.50	7.48

As the 5-parameter model is flexible enough to learn the PV power output at different operating conditions, hourly MPP PV power samples are calculated at other ambient conditions for the whole year, using two main equations, (3.19) and (3.20). Then the necessary number is multiplied with the output to obtain the desired level of PV power for this study to evaluate the reliability of DN. A year output profile of the solar PV power is shown in figure 3.7.

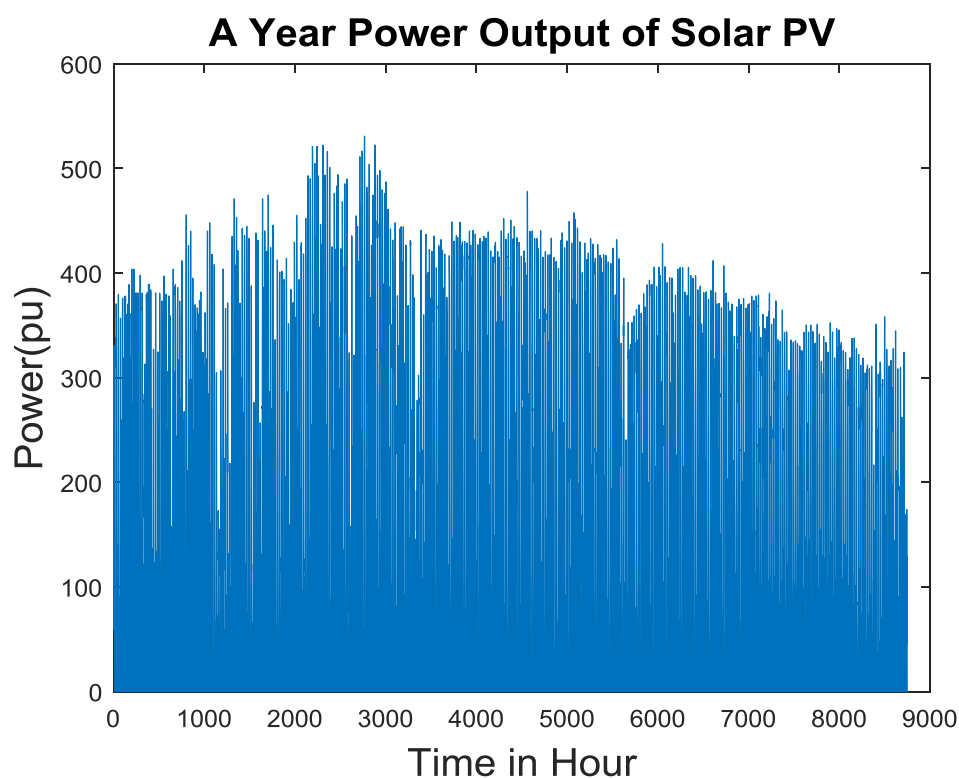


Figure 3.7: Hourly PV Power Output for a Year Using 5-Parameter Model

3.3 Wind DG Model

Wind turbine output power mainly depends on wind speed, expressed by equation (3.22) [44].

$$P_{out}(v) = \begin{cases} 0, & v \leq v_{ci} \cup v \geq v_{co} \\ P_R \frac{v^3 - v_{ci}^3}{v_R^3 - v_{ci}^3}, & v_{ci} < v < v_R \\ P_R, & v \geq v_R \end{cases} \quad (3.22)$$

where

For a specific wind turbine, v_{ci} is the minimum speed for wind power – cut-in speed, v_{co} is the maximum speed for wind power – cut-out speed, v_R is the rated wind speed, P_R is the rated wind power, P_{out} is the output power of that wind turbine and v is the wind speed.

As the wind power is volatile in nature and this work is conducted considering all stochastic conditions, following this practical situation, wind speed is forecasted using the Fuzzy Time Series-Markov Chain forecasting model.

The appropriate parameters for the selected wind turbine are specified and represented in table 3.3.

Table 3.3: Wind Turbine Parameters

v_{ci}	1.2 m/s
v_R	9 m/s
v_{co}	25 m/s
P_R	11 kW

After obtaining the forecasted wind speed, wind power is calculated using equation (3.22). Similar to the consideration of PV power, a desired value of wind power is also considered to evaluate the reliability of DN. A year output profile of the wind power per unit is shown in figure 3.8.

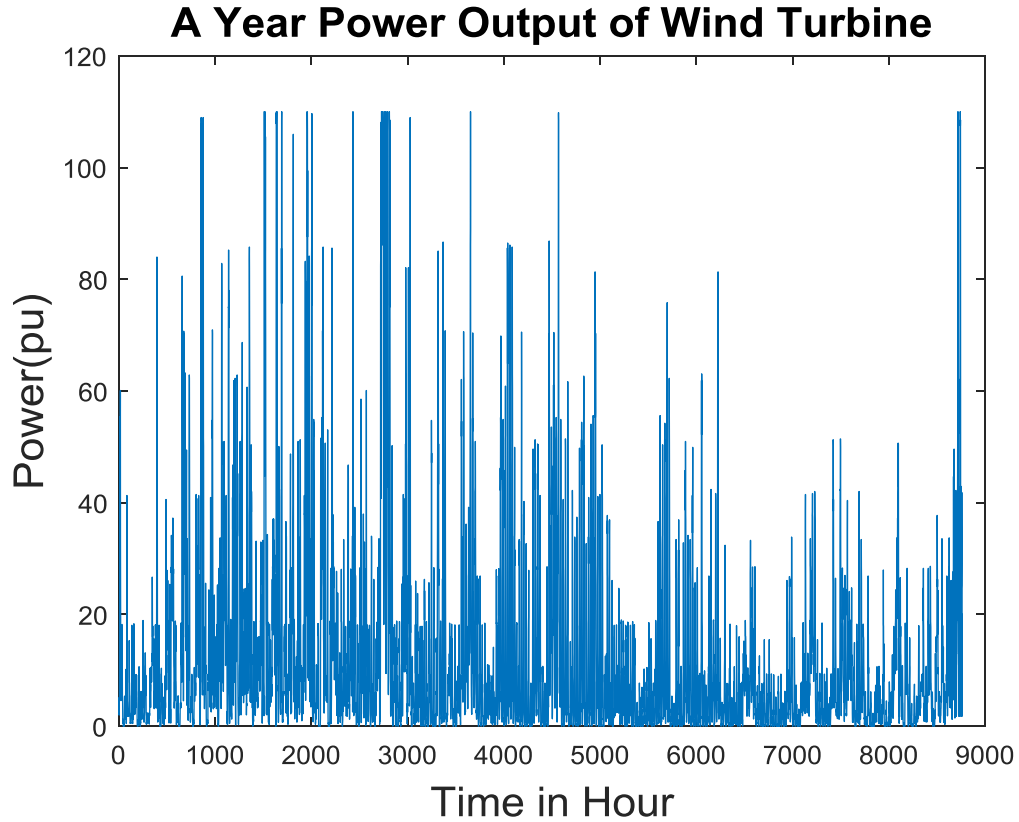


Figure 3.8: Hourly Wind Power Output for a Year

3.4 Load Model

Sequential hourly load for a year will be modeled in this work following the load modeling mechanism explicitly illustrated in reference [99]. According to this approach, historical hourly mean values of the day, daily mean values of the week and weekly mean values of the year are used to form hourly load for the whole year. In this study, seven categories of load are assumed in the IEEE-33 bus distribution system to include the diversity effect (i.e., priority sequence) in the reliability analysis: residential, commercial, industrial, government office, institution, hospital and fire service loads. The hourly mean load values for a year can then be obtained by the following model equation:

$$Mean_k(t) = P_w * P_d * P_h \quad (3.23)$$

where

$Mean_k(t)$ is the historical mean value of k^{th} load at t^{th} hour, P_w, P_d and P_h represent the historical mean values for weeks of year (1,2, ... 52), days of week (1,2,...7) and hours of day (1,2,...24) successively.

After obtaining hourly historical mean values at each load point for a year, the uncertainty of load demand is included, generating mean values of all load points randomly using corresponding historical mean values based on normal distribution function. To comprehend the error between forecasted and actual values in long-term load forecasting that is referred to as about 15% in the literature [100]–[102], 15% of the mean is set equal to the three standard deviations. It does mean that the maximum deviation from mean value can then be no more than 15% if this mean value and standard deviation (SD) are used to generate random samples based on normal distribution function. Equations (3.24) - (3.25) are used to generate hourly random load samples for a year at each load point.

$$3\partial_k(t) = 15\% * Mean_k(t) \quad (3.24)$$

$$L_k(t) = normrnd(Mean_k(t), \partial_k(t)) \quad (3.25)$$

where

$\partial_k(t)$ is the historical SD of k^{th} load at t^{th} hour, $L_k(t)$ is the randomly generated load sample of k^{th} load at t^{th} hour and “normrnd” is the MATLAB command for generating the random value based on normal distribution function.

According to this load modeling technique, total residential load profile and overall load profile for IEEE-33 bus DN are represented in figures 3.9 and 3.10 successively.

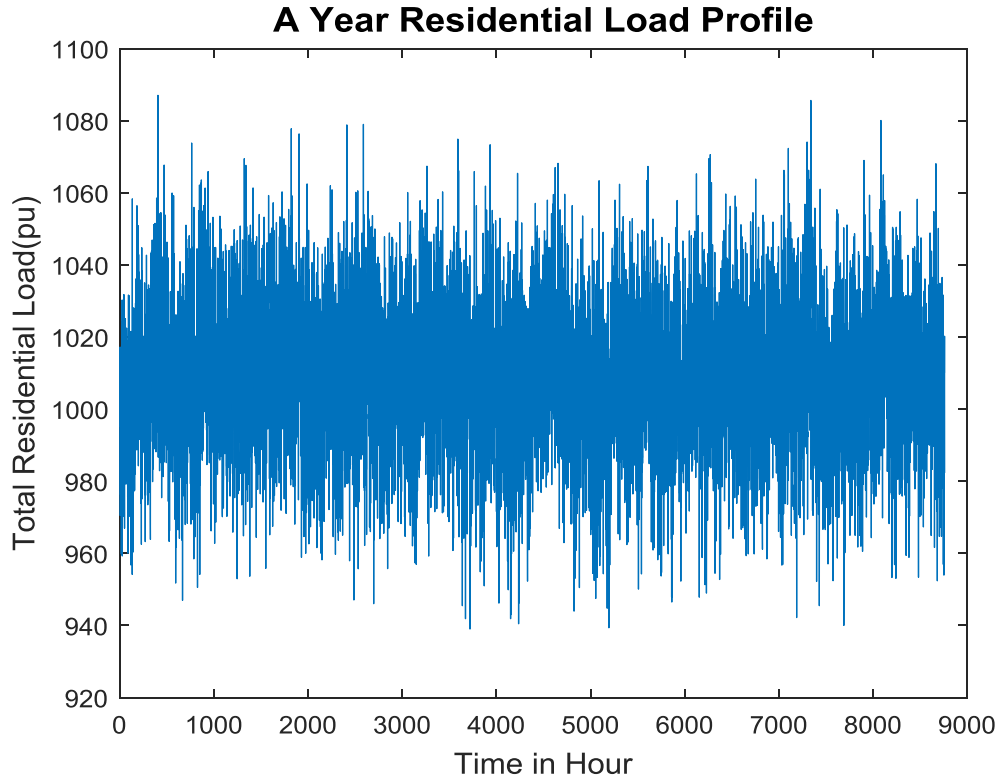


Figure 3.9: Hourly Total Residential Load for a Year on Distribution Network

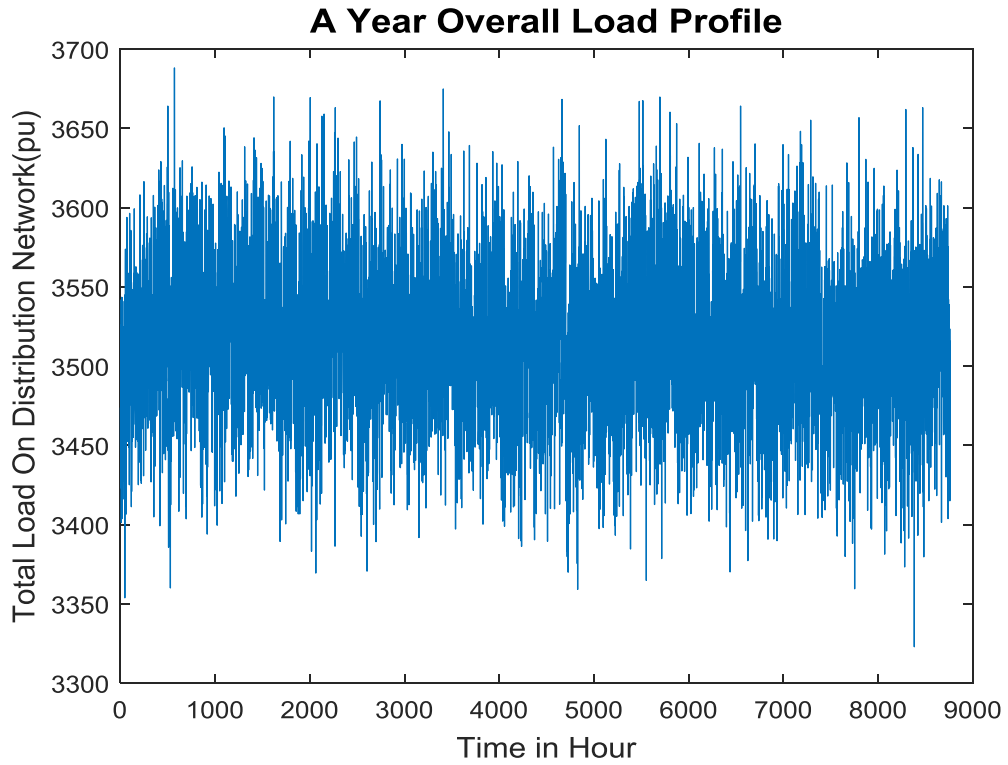


Figure 3.10: Hourly Overall Load for a Year on Distribution Network

3.5 Storage System Model

3.5.1 Modeling Charging-Discharging Procedure of Storage

The probability of storage system charging and discharging for PV-wind-storage combined system power plant depends on the power generated by PV panels and wind turbines and the load required within a specified period of time with the probable conditions of a fully charged and fully discharged storage system. To maintain the charging or discharging mode of the storage system of the PV-wind-storage combined power plant means that the combined system is able to supply the load for this condition. Out of these two conditions, the storage system has the probability of maintaining more three conditions those conditions will determine the availability of the combined system. The PV-wind-storage combined power plant may maintain the condition when the battery is fully charged but the total PV and wind power is more than the load, or it may maintain the condition when the battery is either fully charged or fully discharged or in between but the total PV and wind-generated power is equal to the load power, or it may maintain the condition when the battery is fully discharged but the PV and the wind generate no power. Though these three conditions will not maintain any charging or discharging of the battery, the first two conditions will be able to supply the load whereas the last one will not power the load.

In these conditions, the availability (A) can be defined as the probability (P) of supplying the load (L) by the combined generated PV and wind power or by the storage system or by both within a specified period of time. Therefore, the availability can be represented by equation (3.26).

$$A = P((PV + Wind) \geq L) \cup P(Storage \geq L) \cup P((PV + Wind + Storage) \geq L) \quad (3.26)$$

$$A = P_1 \cup P_2 \cup P_3 \quad (3.27)$$

where

P_1 , P_2 , and P_3 are the respective sequential probabilities used in equation (3.26).

Considering the fully charged and fully discharged conditions of the battery, this availability definition reflects more justified charging or discharging condition of the battery than the availability definition used in [103]. The output of this availability equation will be calculated based on the transferred power between load and PV-wind power generation in the next section. In this case, the full charge of the battery will be partitioned into N discrete states and each state of the battery is defined by the state of charge (SOC). The energy between two adjacent states is separated by an amount of energy Δ as here a one-hour power transferring period is considered for each observation, which will make it easy to represent the battery size and its units in “watt-hours”. As we have considered that the SOC between two adjacent states is separated by Δ , so the energy of any non-integer multiple of Δ including only “0” integer will not cause a transition to the next or previous state for charging or discharging respectively. For example, if $\Delta = 0.002$ (pu) and energy transfer needed from a state is 0.005 or 0.001 (pu), then for 0.005, it will transit two times of Δ , which is equal to 0.004 and the rest of the energy, 0.001, will not cause a transit to the next state, as it is a non-integer of Δ . And in the case of 0.001, it will transit in the same state for the same cause. But in practice, there is always an instantaneous change for charging or discharging except in the full balanced PV-wind power generation with load and the fully charged and discharged conditions which have been mentioned earlier. Because of this complexity due to instantaneous state changing, we have considered discrete states. In this

case, making the choice of the value of Δ as small as possible will closely reflect the instantaneous nature of state changing which has been considered in our availability analysis, as shown in figure 3.11.

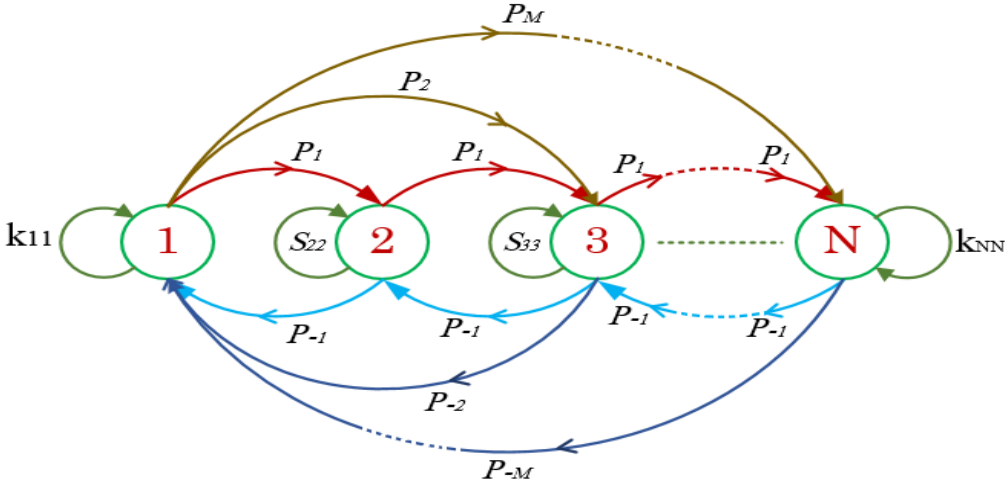


Figure 3.11: Markov-Chain Based Battery Charging-Discharging Transition Diagram

In this case, if we need a larger size of storage for reliability-cost analysis, we can increase the number of states rather choosing the larger Δ .

On the other hand, [103] has considered a discrete number of states but an instantaneous change of state between full charge and full discharge states, which makes all the diagonal elements equal to zero between fully charged and fully discharged states and contradicts its assumption. Because of this, they have made strictly equal the first two elements of the first column and last two elements of the last column of the Markov chain matrix. There may be some conditions when power transfer is less than $|\Delta|$ or zero or near zero, but in all of these cases, they have considered a transition, though their assumption is discrete states for their reliability analysis, which is shown in figure 3.12. As the researchers are looking for availability up to five nines level, they must consider even the balanced PV power generation with the load, though its probability is very low.

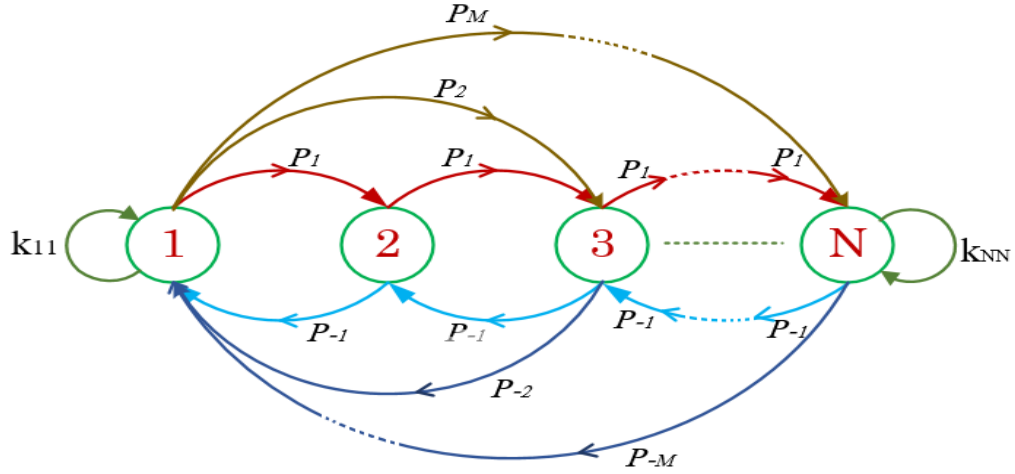


Figure 3.12: Markov-Chain Based Battery Charging-Discharging Transition Diagram [103]

Therefore, after some modifications in case of transiting in the same state, the state space of the charging-discharging storage model for PV-wind-storage system plant can be represented according to discussion and reference [103] as:

$$S = [-M\Delta, -(M - 1)\Delta, \dots, -2\Delta, -\Delta, 0, \Delta, 2\Delta, \dots, (M - 1)\Delta, M\Delta] \quad (3.28)$$

where

The negative sign means that discharging is needed and the positive sign is the opposite case, whereas “0” means that no charging or discharging is necessary – the load and generation are balanced. The storage capacity can then be defined as [103]:

$$C = (N - 1)\Delta T \quad (3.29)$$

where

T is the energy exchanging period for which 1 hour is chosen for simplicity.

According to the state transition diagram in figure 3.11, k_{11} and k_{NN} are the probabilities of staying in state-1 and state-N respectively after the transition in the next time step, which

are the full discharged and charged states. When the battery is in state-1 and the transferring of energy to or from the battery is needed, less than $|\Delta|$ or equal to $-\Delta$ or $-2\Delta \dots$ or $-M\Delta$ or even more than $-M\Delta$ will result in staying in state-1 in the next time step and the same case will occur for k_{NN} but for the opposite condition.

On the other hand, transition in the same state except first and last states will occur when the transferring of energy is less than $|\Delta|$. As a result, the probability of transiting in the same state in the next time step for all states except first and last states will be same and it can be written for figure 3.11 as

$$S_{22} = S_{33} = \dots = S_{(N-1)(N-1)} = Q \quad (3.30)$$

In accordance with the Markov-chain based battery charging-discharging state transition diagram in figure 3.11, the probability of charging energy between any two adjacent states (e.g. probability of charging energy (E) between the ranges $P(\Delta \leq E < 2\Delta)$) is represented by p_1 ; similarly, $p_2 = P(2\Delta \leq E < 3\Delta) \dots p_{M-1} = P((M-1)\Delta \leq E < M\Delta)$ and $p_M = P(E \geq M\Delta)$. Meanwhile, the probability of discharging for the same cases are denoted as $p_{-1}, p_{-2}, \dots, p_{-(M-1)}, p_{-M}$, & $M = N - 1$.

According to the state transition diagram, state of charge (SOC) of a battery can be changed from any of the N states to any of the other states or it can stay in the same state for either charging or discharging within a specified period of time (1 hour for our case). Therefore, the sum of all probabilities for changing SOC from batteries in any state always must be one. The probabilities of energy transferring cause the transition from any of the N states to any of the other states or the same state, whose ‘‘State Space’’ can be written as:

$$PS = [p_{-M}, p_{-(M-1)}, \dots, p_{-2}, p_{-1}, Q, p_1, p_2, \dots, p_{(M-1)}, p_M] \quad (3.31)$$

Therefore, the identity can be written for the probability of transition from any state which represents each row of the transition matrix (N rows for N states) as:

$$p_{-M} + p_{-(M-1)} + \dots + p_{-2} + p_{-1} + Q + p_1 + p_2 + \dots + p_{(M-1)} + p_M = 1 \quad (3.32)$$

Therefore, $N \times N$ order transition probability matrix can be represented by equation (3.33) for the charging-discharging model of the battery where the first column represents the SOC when the battery will enter into fully discharged condition. Then, each Δ amount of energy will be added successively with the current SOC to represent the next SOC till the fully charged state (N^{th} state) is obtained, which represents the last column of the transition matrix.

$$P = \begin{bmatrix} [p_{-M} + p_{-(M-1)} + \dots + p_{-2} + p_{-1} + Q] & \begin{bmatrix} p_1 \\ Q \\ p_{-1} \\ \dots \\ \dots \\ p_{-(M-2)} \\ p_{-(M-1)} \end{bmatrix} & \begin{bmatrix} p_2 \\ p_1 \\ Q \\ \dots \\ \dots \\ p_{-(M-3)} \\ p_{-(M-2)} \end{bmatrix} & \dots & \dots & \begin{bmatrix} p_{M-2} \\ p_{M-3} \\ \dots \\ \dots \\ Q \\ p_{-1} \\ p_{-2} \end{bmatrix} & \begin{bmatrix} p_{M-1} \\ p_{M-2} \\ \dots \\ \dots \\ p_1 \\ Q \\ p_{-1} \end{bmatrix} & \begin{bmatrix} p_M \\ p_{(M-1)} + p_M \\ \dots \\ \dots \\ p_2 + \dots + p_{(M-1)} + p_M \\ p_1 + p_2 + \dots + p_{(M-1)} + p_M \\ Q + p_1 + p_2 + \dots + p_{(M-1)} + p_M \end{bmatrix} \end{bmatrix} \quad (3.33)$$

Therefore, equation (3.33) can be written in the following form of equation (3.34):

$$P = \begin{bmatrix} k_{11} & P_1 & P_2 & \dots & \dots & \dots & P_{M-1} & P_M \\ g_{-1} & Q & P_1 & \dots & \dots & \dots & P_{M-2} & g_{M-1} \\ g_{-2} & P_{-1} & Q & \dots & \dots & \dots & P_{M-3} & g_{M-2} \\ \dots & \dots & \dots & \dots & \dots & \dots & \dots & \dots \\ \dots & \dots & \dots & \dots & \dots & \dots & \dots & \dots \\ g_{-(M-2)} & P_{-(M-3)} & \dots & \dots & \dots & Q & P_1 & g_2 \\ g_{-(M-1)} & P_{-(M-2)} & \dots & \dots & \dots & P_{-1} & Q & g_1 \\ P_{-M} & P_{-(M-1)} & \dots & \dots & \dots & P_{-2} & P_{-1} & P_{NN} \end{bmatrix}_{(3001 \times 3001)} \quad (3.34)$$

where

$$k_{11} = 1 - \sum_{i=1}^M p_i \quad (3.35)$$

$$k_{NN} = 1 - \sum_{i=1}^M p_{-i} \quad (3.36)$$

$$g_{-j} = 1 - (\sum_{i=1}^{j-1} p_{-i} + Q + \sum_{i=1}^M p_i) \quad (3.37)$$

$$g_j = 1 - (\sum_{i=1}^{j-1} p_i + Q + \sum_{i=1}^M p_{-i}) \quad (3.38)$$

where

p_i , p_{-i} & Q will be calculated using energy transferring profile.

According to the Markov chain property, in steady state condition, the limiting probabilities can be obtained using the relation [103]:

$$\pi = \pi P \quad (3.39)$$

Limiting probabilities indicate the Markov chain based charging-discharging procedure to be balanced (fixed) at those probabilities for the corresponding state. These limiting probabilities are used to calculate the loss of load probability (LOLP). The LOLP is the probability of the PV-wind-storage system's unavailability to meet the load, which results in the transition of the battery into fully discharged state within a specified time period. Therefore, the probability of a PV-wind-storage power plant being unable to power the load can then be represented by [103]:

$$p_u = \sum_{i=1}^M [p_{-i} \sum_{k \leq i} \pi_k] \quad (3.40)$$

where

p_u represents the probability of the situation of the PV-wind-storage system when it does not meet the load. If we change the size of the storage by varying either the number of states or Δ or both at the same time this will change the parameters of the equation (3.40). As a result, the probability of unavailability (p_u) will also be changed.

3.5.2 Fuzzy Decision-Making Technique

If the k^{th} Pareto solution of the i^{th} objective function, F_{ki} is represented by the membership function, β_{ki} , then it is defined as

$$\beta_{ki} = \begin{cases} 1, & F_{ki} = F_{ki}^{min} \\ \frac{F_{ki}^{max} - F_{ki}}{F_{ki}^{max} - F_{ki}^{min}}, & F_{ki}^{min} < F_{ki} < F_{ki}^{max} \\ 0, & F_{ki} = F_{ki}^{max} \end{cases} \quad (3.41)$$

where

$k = 1, 2, \dots, \text{No. of Pareto optimal Solutions}$ and $i = 1, 2, \dots, N_{obj}$. F_{ki}^{min} and F_{ki}^{max} are the minimum and maximum value of the i^{th} objective function among the Pareto optimal solutions respectively, and N_{obj} is the number of objective functions. Therefore, the normalized membership function of the k^{th} Pareto optimal solution is written as below:

$$\alpha^k = \frac{\sum_{i=1}^{N_{obj}} \beta_{ki}}{\sum_{k=1}^M \sum_{i=1}^{N_{obj}} \beta_{ki}} \quad (3.42)$$

where

M is the number of Pareto optimal solutions.

3.5.3 Calculation of Transition Probabilities

Based on the predicted data, we calculate the transferred energy at each hour per unit that will fix the transition mode of the battery. In this study, 2.5% of the total predicted hourly load of the IEEE-33 bus DN is considered to be supplied by the PV-wind-storage system whenever an outage will occur whose average at each hour is 60.624 per unit. Therefore, we have considered a PV-wind power plant that generates an average of 123.92 per unit of energy at each hour when looking at 24 hours in each day, but 11 hours are considered to be generated in PV power each day.

The transition probabilities depend on how much power is transferred in each hour and how many times the SOC of storage is changed due to the same amount of power transfer. Transferring of power can then be obtained by subtracting the load from PV-wind power generation for 24 hours in a day. The transferred power can be positive or negative, depending on the amount of power generated by the PV-wind system. The lagging of the PV-wind system is fulfilled by the battery till it becomes fully discharged.

$$P_{transfer} = P_{(PV+wind)} - P_{Load} \quad (3.43)$$

In this case, if transferred power is negative then the battery goes into the discharging mode or the fully discharged mode and if transferred power is positive then the battery goes into the charging mode or the fully charged mode. But for finding the charging-discharging mode of the battery, reference [103] has combined the daytime and nighttime loads, which is not realistic. In addition, the referenced study didn't consider the wind power. However, the histogram of transferred power in figure 3.13 will be used to find the transition probabilities for constructing the state transition matrix in equation (3.34).

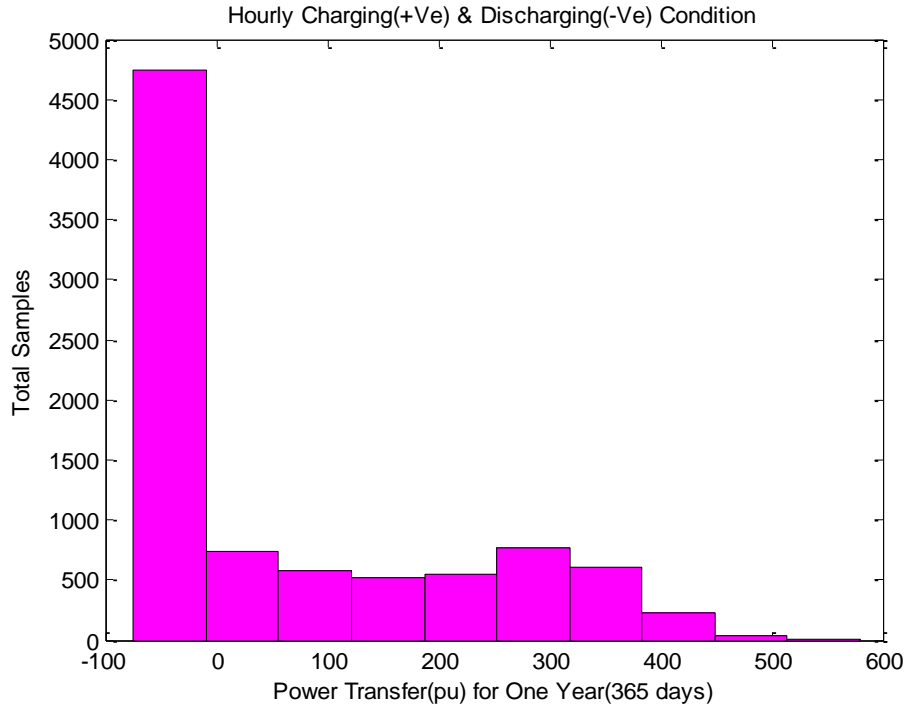


Figure 3.13: Histogram of Power Transfer for 8760 Samples

For instance, if the power transfer takes place in the range $\Delta \leq \text{power transfer} < 2\Delta$ 54 times out of a total 8760 times of power transferring, then the transition probability, p_1 , will be $54/8760 = 0.0062$. In this work, $N = 3001$ states have been considered. Table 3.3 shows the transition probabilities for this work.

Table 3.4: Transition Probability

Probability of transition in same state, $Q = 0.00034247$			
Charging Transition Probabilities (p_i)		Discharging Transition Probabilities (p_{-i})	
p_1	0	p_{-1}	0.0003
p_2	0	p_{-2}	0.0001
.....		
.....		
p_{2999}	0.0001	p_{-2999}	0
p_{3000}	0.0207	p_{-3000}	0

3.5.4 Transition Matrix and Limiting Probabilities

After obtaining the transition probabilities, the transition matrix can be determined using equations (3.35) – (3.38), which is represented by equation (3.44).

$$P = \begin{bmatrix} 0.5523 & 0 & 0 & \dots & 0 & 0.0001 & 0.0207 \\ 0.5519 & 0.0003 & 0 & \dots & 0 & 0 & 0.0208 \\ 0.5516 & 0.0003 & 0.0003 & \dots & 0 & 0 & 0.0208 \\ \dots & \dots & \dots & \dots & \dots & \dots & \dots \\ 0 & 0 & 0 & \dots & 0.0003 & 0 & 0.4477 \\ 0 & 0 & 0 & \dots & 0.0003 & 0.0003 & 0.4477 \\ 0 & 0 & 0 & \dots & 0.0001 & 0.0003 & 0.4481 \end{bmatrix}_{(3001 \times 3001)} \quad (3.44)$$

Whenever we have the transition matrix, we can determine the steady state limiting probabilities using the relation (3.39). In MATLAB, limiting probabilities can be found by increasing the power of the transition matrix till all the rows of the output matrix of the powered transition matrix become the same. Then any row of this output matrix represents the limiting probabilities and any N^{th} element of a row represents the limiting probability of that corresponding SOC. For the best-compromised solution, the limiting probabilities obtained in this work are shown as follows:

$$\pi = [0.0195 \ 0.0000 \ \dots \ \dots \ 0.0002 \ 0.3507]_{1 \times 3001} \quad (3.45)$$

According to the principle of limiting probability mentioned earlier, limiting probability $\pi_{3001} = 0.3507$ means that at steady state, the probability of the fully charged level of battery would be 0.3507 in the Markov chain diagram for the best-compromised solution.

3.5.5 Availability Calculation

According to the definition of availability, it can be written following equation (3.40) as:

$$Availability = 1 - p_u \quad (3.46)$$

In this reliability analysis, availability and storage capacity are found for the best-compromised case to be 0.9547 and 301.721 per unit using equations (3.46) and (3.29) respectively where the time period was 1 hour.

3.5.6 Storage Sizing

In choosing a storage system, decision makers should make an optimal decision between the capacity of the storage and its availability. In this regard, decision makers can vary the parameters of (3.29) to search for their optimal choice. But they may make a mistake in discovering the most compromised solution from many non-dominated possible outcomes.

The objective of storage sizing is to reduce the costs of the PV-wind-storage system power plant while simultaneously reducing the unavailability of the DN, which is a multi-objective optimization problem. As the parameters of equation (3.29) are linearly related to each other, it is possible to obtain the non-dominated Pareto set outcomes, but only a few. The resolution of this possibility will be very high if we increase the number of SOC and decrease the value of power transfer between adjacent states for availability analysis. Change in Δ , even in very small amounts, will have a very high probability of changing at least two state transition probabilities, as the number of states is many. As a result, transition matrix and limiting probabilities will also be changed, which will change the availability as well. That's why this work has chosen the number of SOC as 3001, with 100 small random values of Δ . However, there will still be many possibilities to obtain a few dominated

solutions out of 100 outcomes. However, for simplicity, implementing the complete multi-objective optimization technique with many iterations to find the Pareto front of exact non-dominated solutions rather 100 outcomes obtained in one iteration, which is shown in figure 3.14, is avoided.

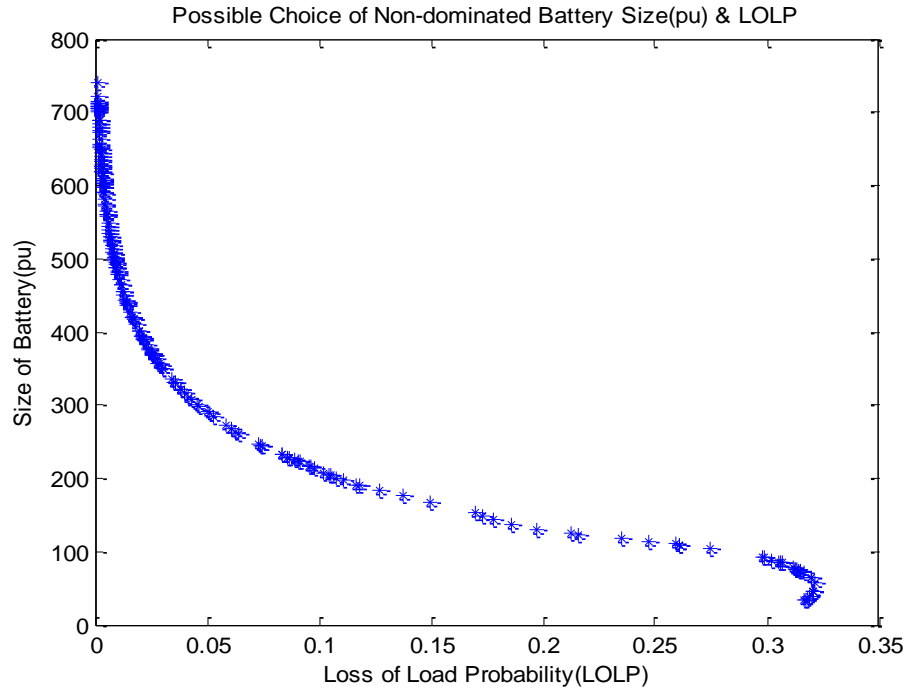


Figure 3.14: Pareto Set of 100 Solutions

Therefore, an assumption is made in this case that all of these outcomes will fulfill the domination conditions as follows: If x^1 and x^2 are two solutions, then there can be two possibilities: one dominates the other or none dominates the other. Maintaining the generality, solution x^1 will dominate solution x^2 if and only if the following two conditions are satisfied:

1. $\forall i \in \{1, 2, \dots, N_{obj}\}: f_i(x^1) \leq f_i(x^2)$
2. $\exists j \in \{1, 2, \dots, N_{obj}\}: f_j(x^1) < f_j(x^2)$

To find the best-compromised solution from this Pareto set, we have adopted two multi-objective concepts to avoid the possibility of a mistake due to choosing in a conventional way.

First, we have implemented the clustering technique to make the Pareto set a manageable size and to increase the possibility of discarding the dominated solutions. A hierarchical clustering algorithm is employed that works iteratively by joining the adjacent clusters until the required number of clusters is obtained based on average linkage technique [104]. The centroid technique is used to find the representatives of the clusters which are the reduced Pareto optimal set, as shown in figure 3.15.

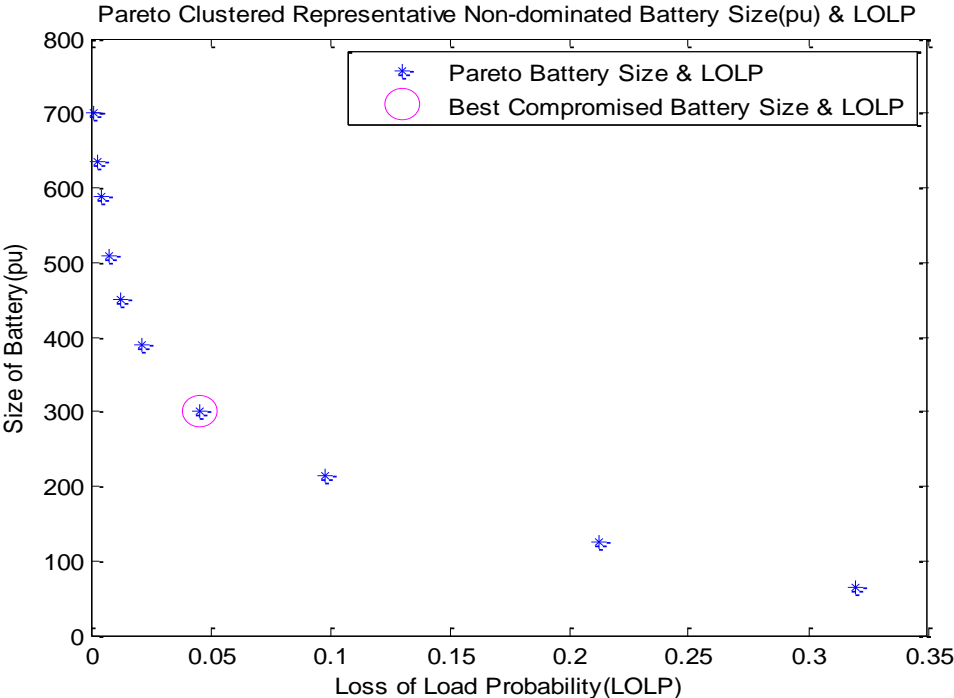


Figure 3.15: Reduced Pareto Optimal Set of Battery Size-Loss of Load Probability (LOLP)

Second, we have implemented the fuzzy decision-making (FDM) technique to find the best-compromised solution from the reduced Pareto optimal set. According to the fuzzy decision-making technique, the best-compromised solution is that having the maximum value of the

normalized membership function, α^k , which is shown in figure 3.15 and figure 3.16 as circled in magenta, for battery size with respect to LOLP and availability respectively.

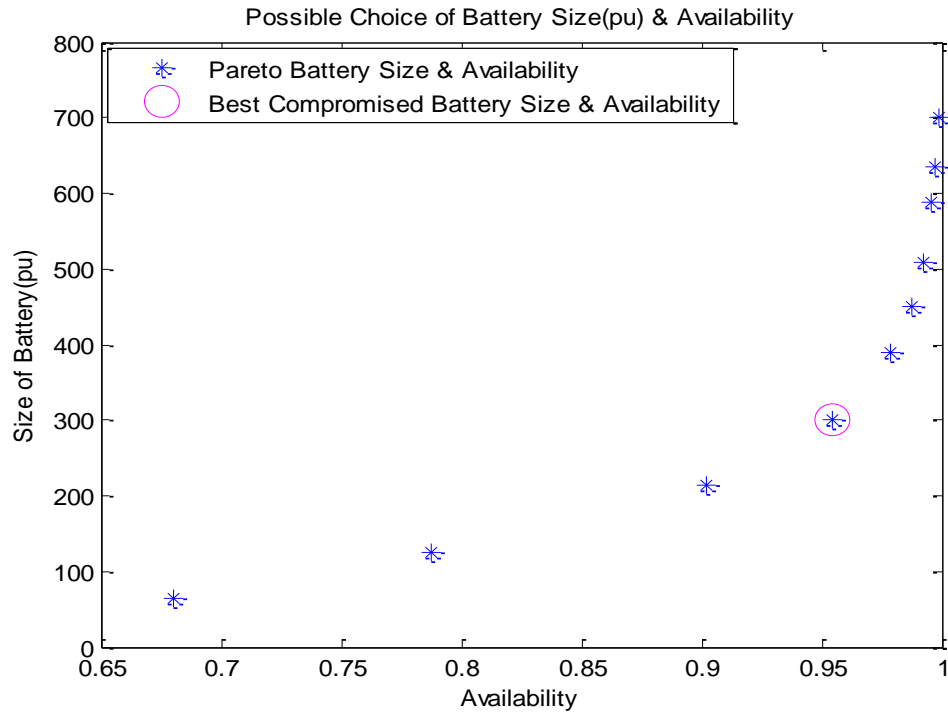


Figure 3.16: Reduced Pareto Optimal Set of Battery Size-Availability

CHAPTER 4

PROBLEM FORMULATION AND METHOD

As the DN reconfiguration problem is a multi-objective, multi-constraints optimization problem, three main objectives in the case of microgrid and four constraints are considered in this optimization fleet to be minimized. Improved Binary Genetic Algorithm (IBGA) is used to solve this problem. In this regard, a single objective function is made, adding weighted values of the three objectives to minimize it using IBGA: Energy Not Supplied (ENS), System Average Interruption Frequency Index (SAIFI) and System Average Interruption Duration Index (SAIDI). The constraints are described as follows:

4.1 Objective Function Formulation

❖ Minimization of Energy Not Supplied (ENS)

The equation used to calculate the ENS at the end of simulation period is written as follows:

$$ENS = \sum_{k=Resolution}^{SP} \sum_{i=1}^n B_i * BusLoad_i * (SP - k + Resolution) * BusCounter_i + \sum_{k=Resolution}^{SP} \sum_{r=1}^m (1 - B) * BusDSMAmount_r * Resolution \quad (4.1)$$

where

$$B_i = \begin{cases} 1; & \text{If load of the } i^{th} \text{ is zero} \\ 0; & \text{If load of the } i^{th} \text{ is not zero} \end{cases}$$

$$BusCounter_i = \begin{cases} 1; & \text{If } i^{th} \text{ bus is not counted before for ENS calculation} \\ 0; & \text{If } i^{th} \text{ bus is counted before for ENS calculation} \end{cases}$$

‘SP’ is the simulation period or faulted period. ‘ $BusLoad_i$ ’ is the amount of forecasted load at the i^{th} bus, ‘n’ is the total number of buses, and ‘Resolution’ is the simulation gap time in the hour between successive simulations. ‘ $BusDSMAmount_r$ ’ is the amount of load considered for DSM implementation at r^{th} bus, meaning that this amount of load will be shed in need owing to paying to those corresponding customers, and ‘m’ is the number of DSM buses.

❖ **Minimization of System Average Interruption Frequency Index (SAIFI)**

The equation used to calculate the SAIFI at the end of simulation period can be written as follows:

$$SAIFI = \frac{\sum_{i=1}^n B_i * N_i}{N_t} \quad (4.2)$$

where

$$B_i = \begin{cases} 1; & \text{If load of the } i^{th} \text{ is zero} \\ 0; & \text{If load of the } i^{th} \text{ is not zero} \end{cases}$$

‘ N_t ’ is the total number of customers in the DN, and ‘ N_i ’ is the number of customers connected at bus ‘i’.

❖ **Minimization of System Average Interruption Duration Index (SAIDI)**

The equation used to calculate the SAIDI at the end of simulation period can be written as follows:

$$SAIDI = \frac{\sum_{i=1}^n U_i * N_i}{N_t} \quad (4.3)$$

where

' N_t ' is the total number of customers in the DN, ' N_i ' is the number of customers connected at bus 'i' and ' U_i ' is the outage time faced by the customers at bus 'i' after any fault in the DN.

In this case, this outage time can be maximum up to the assumed fault period during which the network is reconfigured. After calculating the individual objective functions value, these values are added after multiplying specific weights to be minimized as a single objective function using IBGA. The equation can be written as follows:

$$\text{Min: } f(ENS, SAIFI, SAIDI) = W_1 * ENS + W_2 * SAIFI + W_3 * SAIDI \quad (4.4)$$

where

$$\sum W_1, W_2, W_3 = 1$$

4.2 Constraints

- ❖ Radial Topological structure must be maintained.
- ❖ Power flow through each branch must maintain the maximum limit.

$$P_j \leq P_j^{max} \quad (4.5)$$

where

P_j^{max} is the maximum capacity of power flow through the j^{th} branch and P_j is the amount of power flowing through the j^{th} branch.

- ❖ Bus voltage must lie within the voltage range.

$$V_j^{min} \leq V_j \leq V_j^{max} \quad (4.6)$$

where

V_j^{min} and V_j^{max} are the minimum and maximum permissible voltages of the j^{th} bus successively and V_j is the voltage of the j^{th} bus.

- ❖ DN must supply to the customers following the priority list.

To make this priority list, Monte Carlo Simulation (MCS) is conducted for each branch of IEEE 33 bus DN considering a one-year (8760 hrs) time frame with one-hour resolution time to find the ENS, SAIFI, and SAIDI at each bus. The following figure shows the algorithm of MCS.

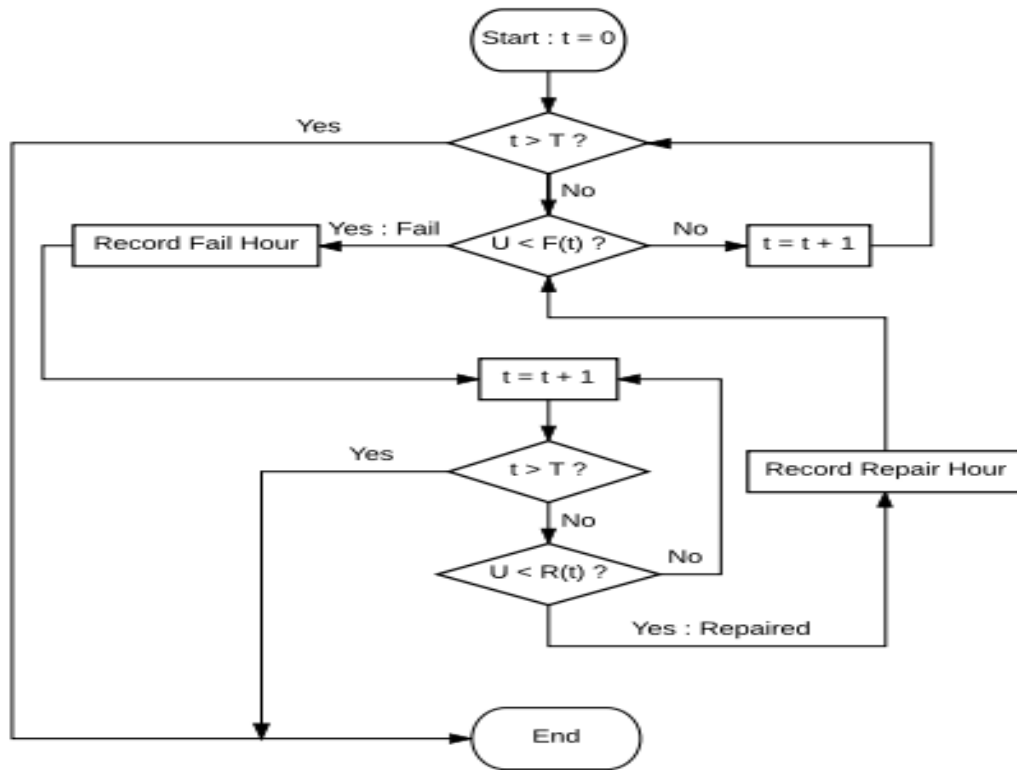


Figure 4.1: Algorithm for Monte Carlo Simulation (MCS)

In this regard, the output of logical ‘and’ for the tie-set of each bus point decides the ‘on’ or ‘off’ state of that corresponding bus point.

4.3 Genetic Algorithm

Improved Binary Genetic Algorithm (IBGA) is used to solve the restoration problem after any fault in the DN where the objective function is minimized following necessary operational constraints. The algorithm has three main operators, which are briefly explained below, to obtain a new child.

4.3.1 Selection

Selection is a process where two parents are selected from many parent solutions for crossover to generate new populations. Two main selection processes are implemented in this study to show the robustness of the technique for solving outage management problem of DN: the random selection and tournament selection.

4.3.2 Crossover

The objective of implementing crossover between two parents is to swap the information and to generate new offspring. After that, depending on the objective function and operational constraints, the better two are selected from the parents and offspring for forwarding to the next, and this procedure ensures the optimal solution. Obvious crossover is always performed in three ways in this work: single point, double point, and uniform crossover, depending on the selected probability of the methods to make it more diversified for convergence.

In this case, single point and double point crossovers are performed by choosing the crossover position(s) randomly; the uniform crossover is performed in a special way

confirming the sum of probabilities of all three crossover methods equal to unity. If ‘alpha’ is the randomly generated chromosome of the same size parent and ‘x1’ and ‘x2’ are the two parents then the following equations ensure the uniform crossover to generate two offspring, ‘y1’ and ‘y2’.

$$\alpha = \text{randi}([0 \ 1], \text{size}(x1)) \quad (4.7)$$

$$y1 = \alpha.* x1 + (1 - \alpha).* x2 \quad (4.8)$$

$$y2 = \alpha.* x2 + (1 - \alpha).* x1 \quad (4.9)$$

where

‘randi’ and ‘size’ are MATLAB commands and ‘.*’ is used in MATLAB for element-by-element multiplication of two matrices.

4.3.3 Mutation

Mutation is performed by flipping one or more gens of a chromosome to increase the biological diversity of that corresponding chromosome. In addition, it sometimes helps to retrieve the lost information. In this study, the one-bit mutation with 100% probability is used but the best one is taken from the mutated and non-mutated ones following objective function values and operational constraints.

CHAPTER 5

RESULTS AND CONCLUSION

5.1 Test System

In order to evaluate the proposed IBGA for restoration service of DN, the following IEEE 33 bus distribution system is considered as a base radial system.

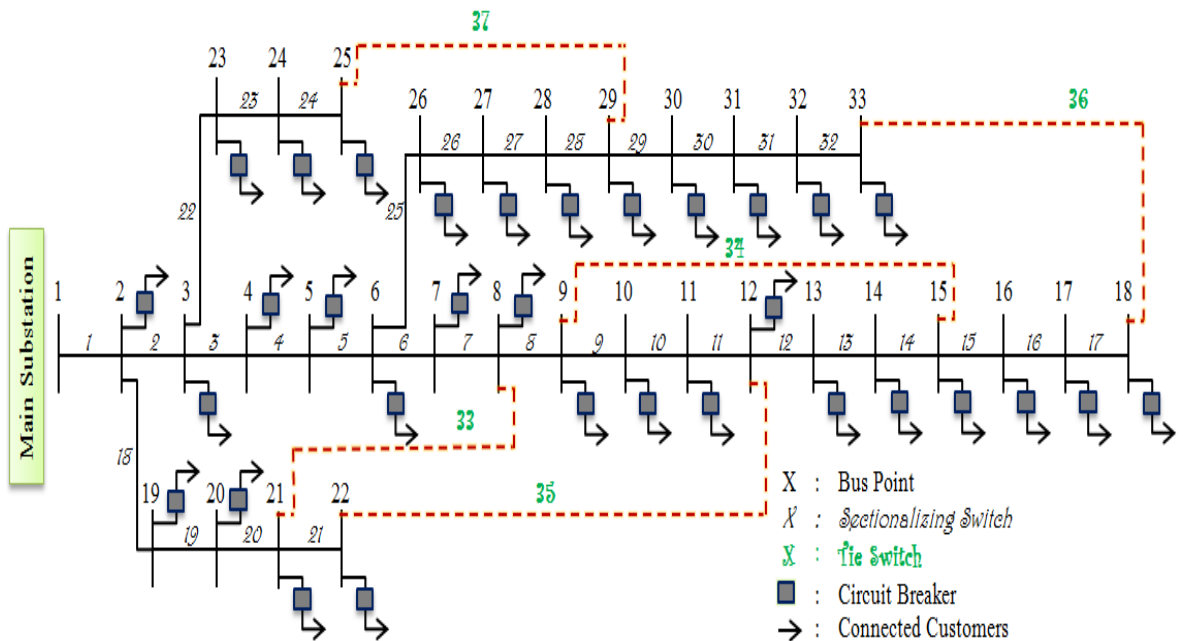


Figure 5.1: IEEE 33 bus distribution system

Following logically, it is assumed that the sectionalizing and tie switches will form different backbone structures of DN in different situations connecting all bus points and maintaining radiality. But the load in each bus is shed, activating the corresponding bus point (BP) circuit breaker so that all bus points are always connected to the substation to maintain the main backbone of the 33-bus system. For this reason, the load of a bus is simply made zero without affecting the connection of that corresponding bus point with the substation in case

of necessity during the restoration process of DN, which is made possible through the circuit breaker activation. In this study, a single fault is considered in case of the branch only when all other possible faults due to the components in other positions (i.e., CBs) are excluded. These faults don't affect the backbone structure of DN to supply power to the customers at healthy bus points through the bus point(s) where the customers are interrupted owing to these excluded faults.

5.2 Type and Number of Consumers

Seven types of consumers are taken into account for this work, where each BP connects a unique consumer type. The types of consumers are mentioned in the table below, with their connecting BPs and number of customers.

Table 5.1: Consumer Types, Numbers and Connecting Bus Information

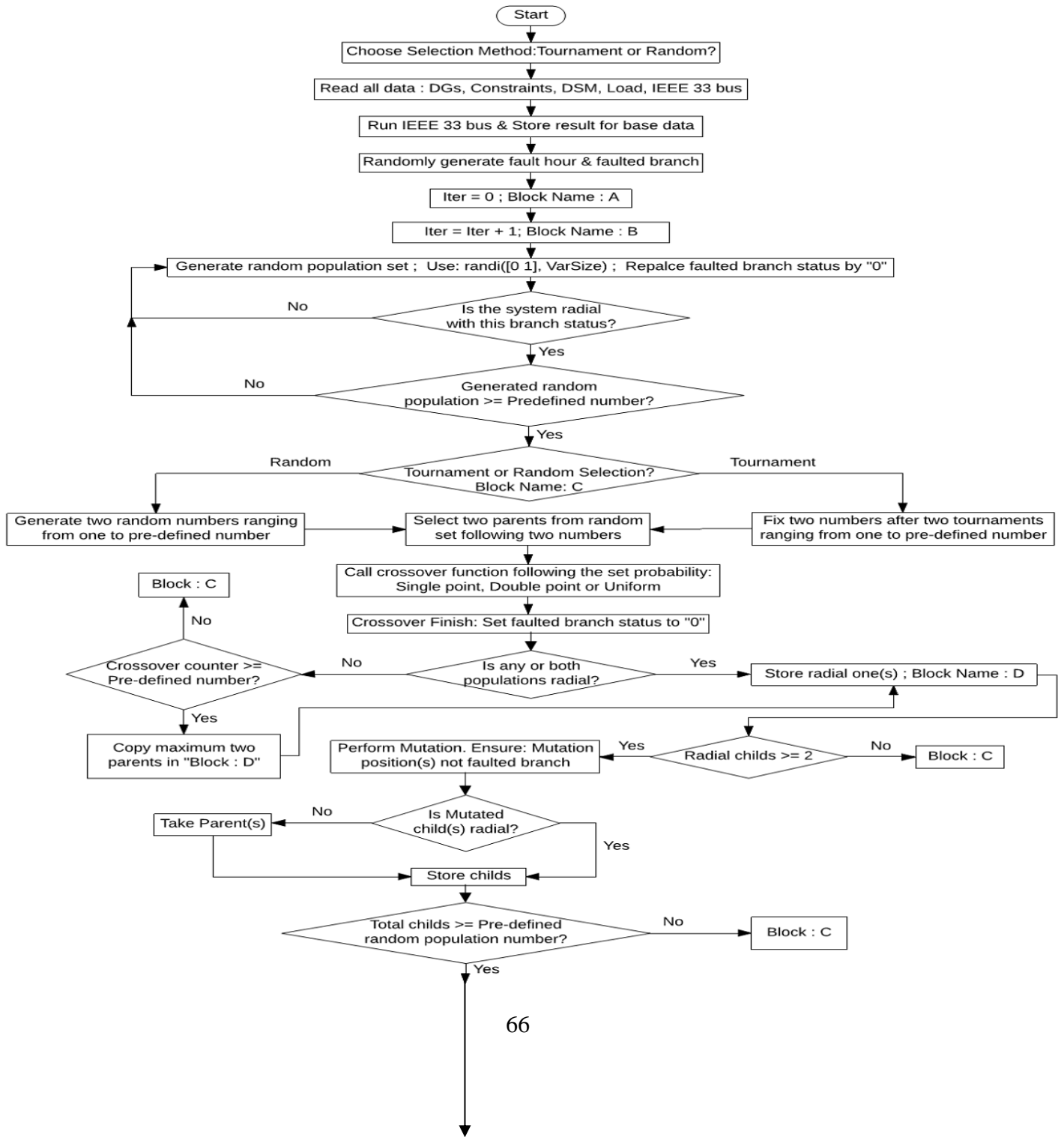
Consumer Type	Connected Bus (Number of Customers)
Residential load	14(150), 15(150), 17(150), 18(150), 26(200), 27(200), 28(200), 30(220), 31(240), 32(210)
Commercial load	5(15), 6(15), 7(15), 8(15), 10(10), 11(10), 12(10)
Industrial load	2(1), 3(1), 4(1), 19(1), 23(1), 24(1), 25(1)
Government office	20(1), 21(1), 22(1)
Institutional load	16(2), 29(1), 33(1)
Fire service	9(1)
Hospital	13(2)

In addition, four buses, 4, 13, 14 and 23, are selected as DSM paying buses, meaning that customers of these buses pay extra money to the utility company to ensure higher reliability, whereas buses, 12, 17 and 25 are considered for the opposite case of DSM, meaning that

they will receive extra money from the company for losing some reliability. In this case, 5% of the historical bus load is taken as the DSM value for that bus.

5.3 Proposed Algorithm for Distribution Network Restoration

To restore the DN after any fault, the proposed algorithm in figure 5.2 is used for implementing the IBGA so that the objective function becomes minimum, maintaining the operational constraints.



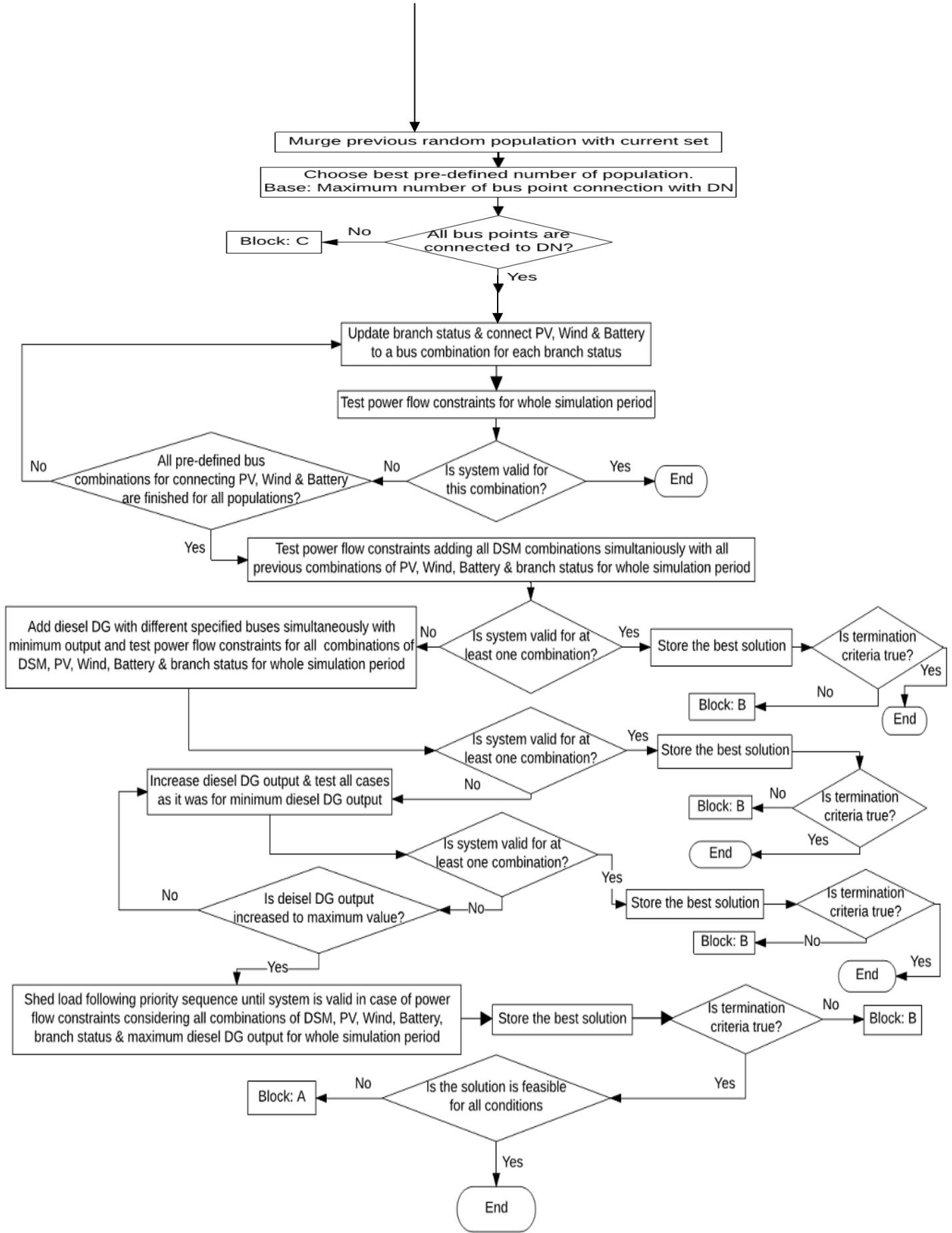


Figure 5.2: Proposed Algorithm for Restoring Loads – the Ultimate Microgrid

According to the flowchart, there are five possibilities to be terminated from the program, ensuring optimal restored DN. For the first case of ending the program, PV power, wind power, and storage system will be enough to restore the DN where no load shedding will occur. In this case, each DG can be connected with a bus out of two bus options; those are 13 and 14, 31 and 32 and 13 and 31 for PV, wind, and battery respectively. If the diesel DG is needed in the optimizing fleet to restore the DN, it can also be connected with one of two bus options, 18 or 23. Thus, the algorithm can restore the faulty network, fulfilling any of the terminating criteria, but sequentially.

5.4 Case Studies

It has already been stated that this thesis work is conducted based on complete probabilistic data considering a one-year mission time for the simulation, with one-hour resolution. Therefore, in order to accumulate the main features of proposed service restoration technique, four cases are considered where the results are obtained at two different hours out of the one-year mission time (MT). In order to optimize the branch status of the DN after fault occurrence, two hours' fault period is chosen in this study. The cases which are tabulated in table 5.2 are described below:

Table 5.2: List of Case Study

Cases	Solar PV	Wind	Storage	Diesel DG	DSM	Load Shedding
Case 1	Included	Included	Included	Not Included	Not Included	Not Included
Case 2	Included	Included	Included	Included	Included	Not Included
Case 3	Included	Included	Included	Included	Included	Included
Case 4	Not Included	Included	Included	Included	Included	Included

5.4.1 Case 1

In case one, the scenario that is considered for analyzing the effectiveness of the proposed algorithm is to restore the distribution network using only three types of DGs – PV, wind, and battery. Since this scenario has no need to include DSM or load shedding features for reconfiguring DN, the value of the objective function will be the minimum, which is zero. For case 1, the fault is taken in branch 21 at the 753rd hour of the year; therefore, continuous optimization is conducted for the 753rd and 754th hours to reconfigure DN for supplying the forecasted loads. Loads at each bus during the outage period are presented in table 5.3.

Table 5.3: Load Values of 33 Buses at 753th & 754th Hours

Bus No.	Load(kW) (753th hour)	Load (kW) (754th hour)	Bus No.	Load (kW) (753th hour)	Load (kW) (754th hour)
1	0	0	18	83.90	86.60
2	97.06	90.84	19	87.89	77.24
3	89.46	85.32	20	89.23	85.08
4	116.46	107.77	21	89.94	80.58
5	54.35	62.53	22	83.45	90.35
6	60.77	57.01	23	90.17	80.55
7	197.41	192.43	24	402.05	429.32
8	193.77	196.14	25	393.26	416.45
9	56.00	56.89	26	51.59	54.63
10	52.79	55.30	27	60.28	55.43
11	44.74	47.21	28	56.89	52.88
12	51.61	48.29	29	125.59	114.54
13	56.61	56.15	30	193.22	193.68
14	107.53	103.31	31	150.00	133.21
15	55.64	55.43	32	192.62	195.42
16	52.84	56.47	33	55.24	55.00
17	57.20	57.60	Total	3549.6	3529.6

To supply this amount of load throughout the faulty period, a simultaneous optimization is conducted to find out the common status of sectionalizing and tie branches for each hour of the faulty period. Similarly, a single bus is optimized for each DG to be connected with it throughout the faulty period, which is practical in theory, but the actual values of the DGs can be different each hour. The results are summarized in table 5.4.

Table 5.4: Results of IEEE 33 Bus Using Tournament Selection

Nth Hour		753	754	Connected Bus	
PV Output (kW)		332.9	411.8	PV	13
Wind Output (kW)		4.2	3.3	Wind	31
Battery Output (kW)		83.4	90.4	Battery	13
Substation Output (kW)		3290.0	3180	
Line Loss (kW)		160.0	153	
Branches Opened		12, 20, 21, 32, 37		Faulted Branch: 21	
Objective Function	Type	Actual ENS (kWh)	Actual SAIFI (Unit less)	Actual SAIDI (hrs)	Weighted Sum of all Obj.
	Value	0	0	0	0

It is observed from table 5.4 that the values of all objective functions are optimized to zero while {12, 20, 21, 32, 37} branches are opened to restore loads where branch 21 is considered to be faulty. In this case, PV and battery are connected with bus point 13; meanwhile, wind DG is connected with bus 31. To restore the total load of 3549.6kW at the 753rd hour, the total contribution of 420.5kW comes from the DGs where PV, wind, and battery are separately supplying 332.9kW, 4.2kW and 83.4kW respectively and the rest of the loads are restored by the substation itself.

It is assumed for all the times that the storage will supply power only when a fault occurs in the system, but PV and wind will supply power to the DN with its full capacity whenever they have availability, as these sources are free of cost. Similarly, for the next hour, part of the load is supplied by PV, wind, and storage, whose amounts are 411.8kW, 3.3kW and 90.4kW respectively. The line losses for a specific resistance of each branch are quantified for this optimal topology in the amount of 160kW and 153kW at the 753rd and 754th hours respectively via load flow analysis. To analyze the superiority and robustness of the proposed algorithm, it is again simulated using a random selection method rather than tournament selection for the same input variable and obtaining the same optimized objective function value but with different connection status. The simulation time for both the selection methods was less than one minute. The results are presented in table 5.5.

Table 5.5: Results of IEEE 33 Bus Using Random Selection

Nth Hour		753	754	Connected Bus	
PV Output (kW)		332.9	411.8	PV	13
Wind Output (kW)		4.2	3.3	Wind	31
Battery Output (kW)		83.4	90.4	Battery	13
Substation Output (kW)		3330.0	3220	
Line Loss (kW)		200.0	193	
Branches Opened		9, 21, 24, 33, 36		Faulted Branch: 21	
Objective Function	Type	Actual ENS (kWh)	Actual SAIFI (Unit less)	Actual SAIDI (hrs)	Weighted Sum of all Obj.
	Value	0	0	0	0

Comparing tables 5.4 and 5.5, it can be concluded that the same amount of load can be restored by different network configurations. Therefore, the main target of this algorithm is to minimize the objective function globally and restore the maximum loads possible using any network configuration from many possibilities within the shortest possible time, which is achieved by this algorithm, proving its robustness.

5.4.2 Case 2

The scenario that is considered for case 2 is to reconfigure the DN, taking the output from all DGs – PV, wind, battery, and diesel – with DSM effect only. In this case, the fault is taken again at the same hour as in case 1 but the faulted branch in this instance is branch number 17. It is already stated in case 1 that all the connection status (i.e., Branch, PV, Wind, and Storage) will be same for the whole faulty period. Similarly, the DSM and the diesel DG are also integrated into the system, considering a common connection status throughout the faulty period. This means that whenever the DSM and diesel DG are considered for specific buses, the effect will continue for the whole simulation period, but the diesel generator can change the output up to the maximum value for reconfiguring optimization. The results for case 2 are summarized in table 5.6.

It is seen from table 5.6 that buses 13, 31, 13 and 18 are optimized for PV, wind, storage, and diesel respectively, whereas the DSM is applied in bus 12 to reconfigure the network for the faulted period while no load shedding is required. Since the DSM comes in optimization fleet for reconfiguring DN, there must be a value of the weighted objective function that is optimized to 0.002.

Table 5.6: Results of IEEE 33 Bus Using Tournament Selection

Nth Hour		753	754	Connected/Applied Bus	
PV Output (kW)		332.9	411.8	PV	13
Wind Output (kW)		4.2	3.3	Wind	31
Battery Output (kW)		83.9	86.6	Battery	13
DSM Value (kW)		3	3	DSM	12
Diesel Output (kW)		200	200	Diesel	18
Substation Output (kW)		3070	2960	
Line Loss (kW)		150	140	
Branches Opened		11, 17, 20, 34, 37		Faulted Branch: 17	
Objective Function	Type	Actual ENS (kWh)	Actual SAIFI (Unit less)	Actual SAIDI (hrs)	Weighted Sum of all Obj.
	Value	6	0	0	0.002

In case of the separate actual value of each objective function, ENS is optimized to 6kWh, while SAIFI and SAIDI are zero as no load shedding is required. In the flow of algorithm, the sequence of the contribution of DGs and DSM for reconfiguring the DN is that PV, wind and storage will be activated at first with the main substation, and the insufficient support of these DGs is caused to implement the DSM, and the diesel DG after that, and finally the load shedding. Although the three buses, {12, 17 and 25} are fixed for implementation of DSM, it is activated only at bus 12, which is an amount of 3kW at each hour, and then the simulation flow turns to the next sequence, which is the inclusion of diesel DG. This is because whenever the total DSM is not sufficient to reconfigure the DN, the diesel generator is taken into account with minimum output and gradually increased to the maximum value. Those values are 200kW and 500kW respectively for this work. Unless any of the diesel DG output with maximum possible DSM can reconfigure the network maintaining all

constraints, the load shedding will be required. Whenever a combination of maximum DSM and a specific diesel DG output becomes able to reconfigure the network, the diesel DG output is no longer increased and then an attempt is made to minimize the DSM value, but at least a minimum value of DSM must be implemented, which is an assumption of proposed algorithm, so that ENS becomes minimum. Thus, the network is optimally reconfigured by opening the branches {11, 17, 20, 34, 37} with 3kW of DSM value, but this is the minimum DSM value chosen for this work, with 200kW of diesel DG output while the PV and wind turbine supply their full capacity. In this case, the output of the battery is 83.9kW and 86.6kW during the outage period successively. Using the power flow solution, line losses are quantified to 150kW and 140kW successively for this topology during the outage period. Again, the topology is simulated with same input but changing the selection method of IBGA, and the obtained results are tabulated in table 5.7.

Table 5.7: Results of IEEE 33 Bus Using Random Selection

Nth Hour		753	754	Connected/Applied Bus	
PV Output (kW)		332.9	411.8	PV	13
Wind Output (kW)		4.2	3.3	Wind	31
Battery Output (kW)		83.9	86.6	Battery	13
DSM Value (kW)		3	3	DSM	12
Diesel Output (kW)		200	200	Diesel	18
Substation Output (kW)		3110	3010	
Line Loss (kW)		190	181	
Branches Opened		12, 17, 20, 24, 33		Faulted Branch: 17	
Objective Function	Type	Actual ENS (kWh)	Actual SAIFI (Unit less)	Actual SAIDI (hrs)	Weighted Sum of all Obj.
	Value	6	0	0	0.002

Similar to case 1, it is again observed from table 5.7 that the algorithm is robust and superior to find any of the possible optimal topologies. In addition, the same amount of diesel DG output and DSM are optimized for both selection methods.

5.4.3 Case 3

In this case study, the scenario that is considered is to reconfigure the DN when all the DGs, DSM effect and load shedding are needed owing to an interruption in branch 5 at the 3585th hour. To investigate the effectiveness of this algorithm for restoring loads, loads at each bus during the faulted period are forecasted and are presented in table 5.8.

Table 5.8: Load Values of 33 Buses at 3585th & 3586th Hours

Bus No.	Load(kW) (3585 th hour)	Load (kW) (3586 th hour)	Bus No.	Load (kW) (3585 th hour)	Load (kW) (3586 th hour)
1	0	0	18	86.05	78.83
2	96.23	89.55	19	80.31	85.84
3	85.05	93.89	20	82.19	83.36
4	120.33	109.84	21	91.97	87.27
5	56.47	56.94	22	89.29	84.57
6	57.95	56.80	23	83.28	87.46
7	180.63	191.22	24	381.07	376.08
8	185.32	215.26	25	397.82	390.84
9	55.47	59.46	26	53.89	55.88
10	54.12	57.25	27	56.79	54.26
11	47.36	41.60	28	56.89	52.88
12	57.66	53.48	29	125.59	114.54
13	54.25	61.14	30	193.22	193.68
14	111.44	116.51	31	150.00	133.21
15	61.85	59.62	32	192.63	195.42
16	52.80	56.76	33	55.24	55.00
17	57.19	51.90	Total	3510.3	3500.3

To assess the performance of the proposed algorithm when allocation of all DGs in specific locations and implementation of DSM can't fulfill the operational constraints to find an optimal reconfigured candidate topology for the forecasted loads in table 5.8, simultaneous simulation is conducted, including a load shedding feature. Then the optimal reconfigured candidate topology is obtained and a summary provided in table 5.9.

Table 5.9: Results of IEEE 33 Bus Using Tournament Selection

Nth Hour		3585	3586	Connected/Applied Bus	
PV Output (kW)		400.4	424.6	PV	13
Wind Output (kW)		53.9	40.4	Wind	31
Battery Output (kW)		156.5	156.5	Battery	13
DSM Value (kW)		0	0	DSM	--
Diesel Output (kW)		500	500	Diesel	23
Substation Output (kW)		440	400	
Line Loss (kW)		90	87	
Shed Buses		2, 3, 4, 5, 6, 7, 8, 10, 11, 12, 19, 23, 24, 25, 26, 27, 28	2, 3, 4, 5, 6, 7, 8, 10, 11, 12, 19, 23, 24, 25, 26, 27, 28	
Branches Opened		5, 7, 8, 11, 35		Faulted Branch: 5	
Objective Function	Type	Actual ENS (kWh)	Actual SAIFI (Unit less)	Actual SAIDI (hrs)	Weighted Sum of all Obj.
	Value	4120.24	0.353	0.705	1.75

Simulating the DN simultaneously using the proposed algorithm throughout the faulted period, the optimal reconfigured candidate topology is found by opening branches {5, 7, 8,

11, 35} and connecting the DGs, PV, wind, storage and diesel at buses {13, 31, 31, 23} successively. The algorithm has shown successful optimization of the value of DSM, which is zero in this case, and the optimal DG connection buses for this optimal candidate network. One of the constraints that is maintained for reconfiguring DN is priority sequence. Whenever the bus(es) needs to be shed in the reconfiguration simulation, the bus which is shed first is the bus of lowest priority and next ones accordingly. In this work, the priority list is made on an hourly basis for the buses.

To maintain a priority list for this work, an assumption is made that whenever a fault occurs in the network at a specific hour, the priority list for that specific hour will be followed for the whole faulty period to reconfigure the network. For instance, since the fault is taken at the 3585th hour, the priority list of the 3585th hour will be maintained at hours 3585 and 3586, for shedding the bus(es) to reconfigure DN. The priority list for the 3585th hour is listed in table 5.10, where the priority is decreased from left to right.

Table 5.10: Priority List for Buses

Bus No.	13	16	29	9	33	21	20	22	32	31	18	30	14	17	15	25	→
→	27	26	11	3	28	24	8	10	2	12	19	6	5	4	23	7	

The strategy of shedding the buses is considered in this work is that whenever a bus is shed, it is continued for the whole faulty period, as the customers will not prefer a frequent on/off from the utility. This is why it is seen from table 5.9 that the total 17 common buses are shed in each hour during the outage period when the priority sequence is maintained. In this case, the diesel DG supplies its maximum capacity, 500kW, to reduce the number of the shed buses. The other DGs – PV, wind and storage – meanwhile supply power to the

network at the 3585th and 3586th hours which, amounts to {400.4kW, 53.9kW and 156.5kW} and {424.6kW, 40.4kW and 156.5kW} successively. The line losses for this topology are simulated to 90kW and 87kW successively during the faulted period. The optimal topology is shown in figure 5.3.

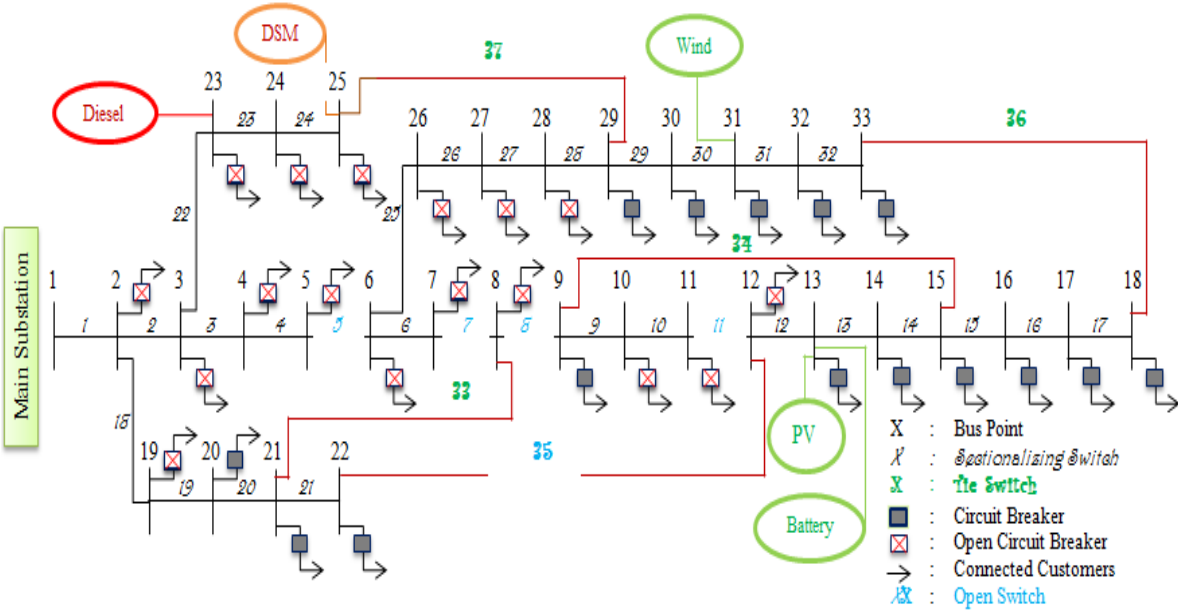


Figure 5.3: Optimal Reconfigured Microgrid Network for Case 3

In this topology, ENS, SAIFI, and SAIDI are optimized to 4120.24kWh, 0.353, and 0.705hrs successively, whereas the weighted scalar objective function that is actually optimized by the algorithm is 1.75.

5.4.4 Case 4

To investigate the effect of the microgrid (MG) concept in DN, case 4 is considered as a reflection of case 3, with similarity of all the input variables apart from PV output, which is forcedly made zero in both hours of the faulty period and its output evaluated. In this case, some comparisons are made with case 3.

Therefore, it is assumed that the fault occurs at the 3585th hour in branch 5. The results obtained using the proposed algorithm are provided in table 5.11.

Table 5.11: Results of IEEE 33 Bus Using Tournament Selection

Nth Hour		3585	3586	Connected/Applied Bus	
PV Output (kW)		0	0	PV	13
Wind Output (kW)		53.9	40.4	Wind	31
Battery Output (kW)		156.5	156.5	Battery	13
DSM Value (kW)		0	0	DSM	--
Diesel Output (kW)		500	500	Diesel	23
Substation Output (kW)		580	800	
Line Loss (kW)		60	70	
Shed Buses		2, 3, 4, 5, 6, 7, 8, 10, 11, 12, 14, 15, 17, 19, 23, 24, 25, 26, 27, 28	2, 3, 4, 5, 6, 7, 8, 10, 11, 12, 14, 15, 17, 19, 23, 24, 25, 26, 27, 28	
Branches Opened		5, 6, 11, 35, 36		Faulted Branch: 5	
Objective Function	Type	Actual ENS (kWh)	Actual SAIFI (Unit less)	Actual SAIDI (hrs)	Weighted Sum of all Obj.
	Value	4578.75	0.58	1.16	2.131

Buses optimized for connecting DGs in case 4 are {13, 31, 13 and 23} for PV, wind, battery, and diesel DG successively. The wind and battery output are same as in case 3, and the output of the diesel DG is optimized to 500kW for the same reason as in case 3; meanwhile, the DSM value is optimized to zero.

It is seen from table 5.11 that 20 common buses are shed in both hours to find the optimal reconfigured candidate topology whose five open branches are {5, 6, 11, 35, 36}. The topology for case 4 is depicted in figure 5.4.

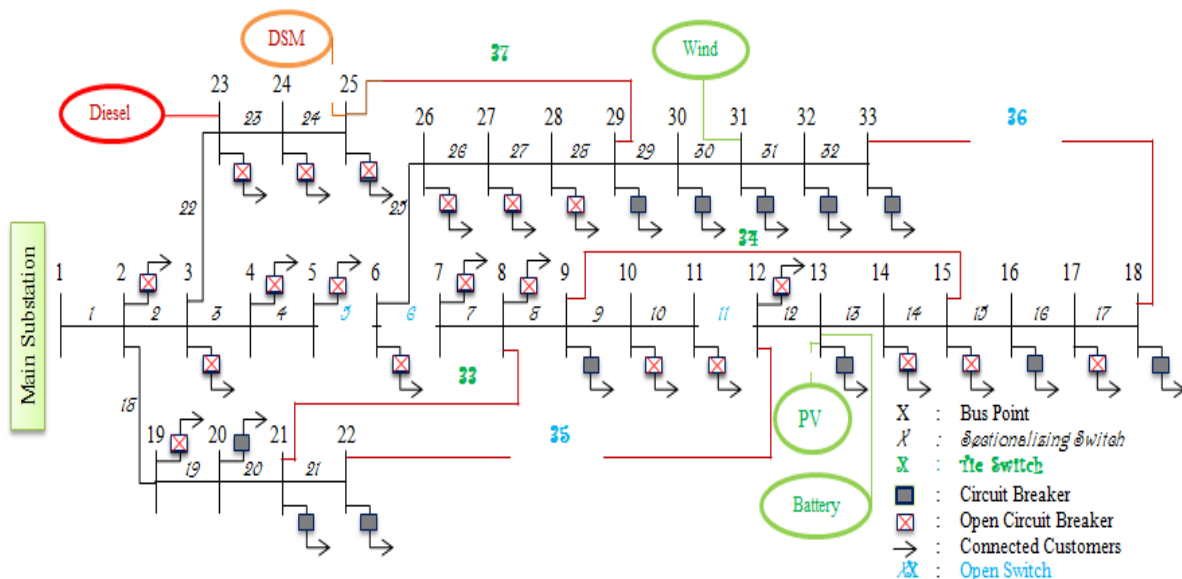


Figure 5.4: Optimal Reconfigured Network for Case 4

It can be noticed from the figure that the five branches are always opened for maintaining the radiality of the network. However, buses for the DSM implementation are automatically ignored, as all the DSM implementation buses have already been included in the shed buses. Using the power flow simulation, the line losses for case 4 are quantified to 60kW and 70kW successively during the faulted period.

One of the important features of DN to be considered a MG is to include the distributed source(s) (i.e., PV, wind, etc.) in the network to improve its service. This MG feature can be investigated from tables 5.8, 5.9 and 5.11. ENS for case 3 is 4120.24kWh, whereas the ENS for case 4 is 4578.75kWh and the large difference of ENS, 458.51kWh, between these two cases is due to not supplying the power by PV source throughout the faulty period. It is

because the unavailability of PV power results in more buses to be shed, though the substation had the capacity of an equivalent amount of lost PV power to optimize a reconfigured candidate topology. In this case, it can be said that an 11.13% increase in performance is possible by including the microgrid concept in DN. Similarly, reliability will also be improved in DN due to converting it to a microgrid network in case of SAIFI and SAIDI that is seen from tables 5.9 and 5.11.

It is worthwhile to mention that there is always a dilemma in iterative method between simulation time and converging exactly in the optimal location. This means that when the number of iterations is increased, the simulated solution will come very close to the exact optimal solution or be the exact optimal solution and vice versa. However, the time required to optimize these reconfigured networks is less than one minute.

Finally, it can be stated from the above discussion that the proposed algorithm can handle the installation of all types of DGs and implementation of DSM with proper sizing and siting and the scheduling of load shedding in a proper way by optimizing a reconfigured candidate network for a specific fault period. The algorithm also optimally proves the importance of converting the DN to a microgrid network to increase the network's reliability.

CHAPTER 6

CONCLUSIONS AND FUTURE WORK

6.1 Conclusions

Microgrid has a great impact on providing reliable service to the customers via reducing the indices, ENS, SAIFI, and SAIDI. But an algorithm needs to be developed to manage the energy of distributed sources and conventional power from the substation among loads of microgrid after occurring outages in the network via an optimal reconfigured topology of the microgrid. In this case, least or zero amount of DSM energy and/or the minimum number of bus(s) or no buses to be shedded are optimized for fulfilling the constraints. Therefore, an improved binary genetic algorithm (IBGA) based optimization technique has been developed in this work. Four types of DGs – PV, wind, storage, and diesel generator have been considered to improve the reliability of microgrid. As this work is completely based on stochastic data, three DGs – PV, wind and storage, and load are modeled stochastically whereas some sample values are considered as the output of diesel DG. However, the flow of this proposed algorithm is considered in such a way that it first tries to mitigate fault in the network via an optimal reconfiguration using PV, wind, and storage. In case of failing to find an optimal configuration using these three DGs, the algorithm includes DSM and similarly the diesel DG after that. Finally, the proposed algorithm gradually sheds the busloads in needs following priority list till an optimal reconfiguration is obtained. Though this restoration problem is a multi-objective, multi constraints problem, specific weights are multiplied with objectives and then the objectives are summed together

to make a scalar form minimization problem. Sizing and siting of DGs and DSM both are considered in minimizing objective function to find optimal topology ensuing full capacity supply from PV and wind DGs. The algorithm shows superiority to optimize reconfigured topology after fault via minimizing multi-objectives in scalar form.

6.2 Future Work

The suggestions for the future work are given below:

- ❖ Following four constraints, three objectives are indexed as a standard for optimally reconfiguring microgrid (MG) to improve reliability but power loss. Hence, power loss can be included as an additional objective or constraint.
- ❖ Although the locations and sizes of DGs are optimized to manage power properly among the buses of MG, each DG is treated as a single unit that limits the number of locations for connecting DGs with many buses and variation of DG outputs. Therefore, further improvement is possible considering a number of units of different size for each DG to be connected with many buses.
- ❖ The feature of reducing the number of switching operations in case of connecting DGs, changing branch statuses, implementation of DSM can be included which will reduce the time for changing the old configuration to the new one at all.
- ❖ The proposed algorithm can be simulated in the real-time digital simulator (RTDS) that will be the previous step of stepping into the real system.

References

- [1] L. Jin, D. Cong, L. Guangyi and Y. Jilai, “Short-term net feeder load forecasting of microgrid considering weather conditions,” *ENERGYCON 2014 - IEEE Int. Energy Conf.*, pp. 1205–1209, 2014.
- [2] A. Ouammi, H. Dagdougui and R. Sacile, “Optimal Control of Power Flows and Energy Local Storages in a Network of Microgrids Modeled as a System of Systems,” *IEEE Trans. on Control Systems Technology*, vol. 23, no. 1, pp. 128–138, 2015.
- [3] A. Oualle, G. Ramos, S. Bacha, A. Hably and A. Rumeau, “Decentralized control of Voltage Source Converters in Microgrids based on the Application of Instantaneous Power Theory,” *IEEE Trans. Ind. Electron.*, vol. 62, no. 2, pp. 1152–1162, 2014.
- [4] W. Jiangbo, B. Zhiwen, Z. Xiaoman and Li Zheng “A low-voltage Micro-grid Control Method Based on Standardized Information Model ,” *2014 IEEE Workshop on Electronics , Computer and Applications*, pp. 1027–1031, 2014.
- [5] J. M. Guerrero, M. Chandorkar, T. L. Lee and P. C. Loh, “Advanced Control Architectures for Intelligent Microgrids—Part I: Decentralized and Hierarchical Control,” *IEEE Trans. Ind. Electron.*, vol. 60, no. 4, pp. 1254–1262, 2013.
- [6] J. A. Cohen, J. L. Edwards and C. Marnay, “Ernest Orlando Lawrence Berkeley National Laboratory U . S . Regional Energy Demand Forecasts Using NEMS and GIS,” *Enviornmental Energy Technologies Devision*, 2005.
- [7] D. Cheng and B. Venkatesh, “Literature survey and comparison of consumer interruption costs in North America and Europe,” *Can. Conf. Electr. Comput. Eng.*, pp. 1–7, 2014.
- [8] R. E. Brown, Jiuping Pan, Xiaorning Feng and K. Koutlev, “Siting distributed generation to defer T&D expansion,” *2001 IEEE/PES Transmission and Distribution Conference and Exposition. Developing New Perspectives (Cat. No.01CH37294)*, pp. 622–627, 2001.
- [9] Saeed Teimourzadeh, Farrokh Aminifar, Mahdi Davarpanah and Josep M. Guerrero “Macroprotections for Microgrids: Toward a New Protection Paradigm Subsequent to Distributed Energy Resource Integration,” *IEEE Industrial Electronics Magazine*, vol. 10, no. 3, pp. 6–18, 2016.

- [10] Qiang Fu, Luis F. Montoya, Ashish Solanki, Adel Nasiri, Vijay Bhavaraju, T. Abdallah and David C. Yu, “Microgrid Generation Capacity Design With Renewables and Energy Storage Addressing Power Quality and Surety,” *IEEE Transactions on Smart Grid*, vol. 3, no. 4, 2012.
- [11] Huang Wei, He Zijun, Feng Li, Tian Hongliang and Zhang Li, “Reliability Evaluation of Microgrid with PV-WG Hybrid System,” *2011 4th International Conference on Electric Utility Deregulation and Restructuring and Power Technologies (DRPT)*, pp. 1629–1632, 2011.
- [12] W. Wangdee, “Reliability Impact of Intermittent Renewable Energy Source Integration into Power System,” *2014 International Electrical Engineering Congress (iEECON)*, pp. 1–4, 2014.
- [13] J. Skea, D. Anderson, T. Green, R. Gross, P. Heptonstall and M. Leach, “Intermittent renewable generation and the cost of maintaining power system reliability,” *IET Generation, Transmission & Distribution*, vol. 2, no. 1, pp. 82–89, 2008.
- [14] Q. Zhao, P. Wang, L. Goel and Y. Ding, “Impacts of Renewable Energy Penetration on Nodal Price and Nodal Reliability in Deregulated Power System,” *2011 IEEE Power and Energy Society General Meeting*, pp. 1–6, 2011.
- [15] C. Singh and A. Lago-Gonzalez, “Reliability Modeling of Generation Systems Including Unconventional Energy Sources,” *IEEE Transactions on Power Apparatus and Systems*, vol. PAS-104, no. 5, pp. 1049–1056, 1985.
- [16] E. Yao, P. Samadi, V. W. S. Wong and R. Schober, “Residential Demand Side Management Under High Penetration of Rooftop Photovoltaic Units,” *IEEE Transactions on Smart Grid*, vol. 7, no. 3, pp. 1597–1608, 2016.
- [17] M. Davoudi, V. Cecchi and J. R. Ag, “Network Reconfiguration with Relaxed Radiality Constraint for Increased Hosting Capacity of Distribution Systems,” *2016 IEEE Power and Energy Society General Meeting (PESGM)*, pp. 1–5, 2016.
- [18] M. Nuri, M. R. Miveh, S. Mirsaedi and M. R. Gharibdoost, “Distributed Generation Placement to Maximize the Loadability of Distribution System Using Genetic Algorithm,” *2012 Proceedings of 17th Conference on Electrical Power Distribution*, 1–5, 2012.
- [19] A. K. Bohre, G. Agnihotri and M. Dubey, “Optimal sizing and sitting of DG with load models using soft computing techniques in practical distribution system,” *IET Generation, Transmission & Distribution*, vol. 10, no. 11, pp. 2606–2621, 2016.

- [20] R. J. C. Gallano and A. C. Nerves, "Multi-objective Optimization of Distribution Network Reconfiguration with Capacitor and Distributed Generator Placement," *TENCON 2014 - 2014 IEEE Region 10 Conference*, pp. 1–6, 2014.
- [21] R. H. Fayek and R. A. Sweif, "AI based Reconfiguration Technique for Improving performance and operation of Distribution Power Systems with Distributed Generators," *4th International Conference on Power Engineering, Energy and Electrical Drives*, pp. 215–221, 2013.
- [22] R. S. Rao, K. Ravindra, K. Satish and S. V. L. Narasimham, "Power Loss Minimization in Distribution System Using Network Reconfiguration in the Presence of Distributed Generation," *IEEE Transactions on Power Systems*, vol. 28, no. 1, pp. 317–325, 2013.
- [23] Aboelsood Zidan and E. F. El-Saadany, "Service Restoration in Balanced and Unbalanced Distribution Systems with High DG Penetration," *2011 IEEE Power and Energy Society General Meeting*, pp. 1–8, 2011.
- [24] P. Alinezhad, O. Z. Bakhoda and M. B. Menhaj, "Optimal DG placement and capacity allocation using intelligent algorithms," *2015 4th Iranian Joint Congress on Fuzzy and Intelligent Systems (CFIS)*, pp. 1–8, 2015.
- [25] E. Yao, P. Samadi, V. W. S. Wong and R. Schober, "Residential Demand Side Management Under High Penetration of Rooftop Photovoltaic Units," *IEEE Transactions on Smart Grid*, vol. 7, no. 3, pp. 1597–1608, 2016.
- [26] M. Fotuhi-Firuzabad and R. Billinton, "Impact of Load Management on Composite System Reliability Evaluation Short-Term Operating Benefits," *IEEE Transactions on Power Systems*, vol. 15, no. 2, pp. 858–864, 2000.
- [27] R. Billinton and D. Lakhanpal, "Impacts of demand-side management on reliability cost/reliability worth analysis," *IEE Proceedings - Generation, Transmission and Distribution*, vol. 143, no. 3, pp. 225–231, 1996.
- [28] M. Zhou, G. Li and P. Zhang, "Impact of Demand Side Management on Composite Generation and Transmission System Reliability," *2006 IEEE PES Power Systems Conference and Exposition*, pp. 819–824, 2006.
- [29] R. Azami and A. F. Fard, "Impact of Demand Response Programs on System and Nodal Reliability of a Deregulated Power System," *2008 IEEE International Conference on Sustainable Energy Technologies*, pp. 1262–1266, 2008.
- [30] A. Gabaldbn, A. Molina, C. Roldan, J. A. Fuentes, E. Gbmez, P. Lara, J. A. Dominguez and E. Tarancbn, "Assessment and Simulation of Demand-Side

- Management Potential in Urban Power Distribution Networks,” *2003 IEEE Bologna Power Tech Conference Proceedings*, pp. 1–5, 2003.
- [31] S. Acharya, M. Shawky El Moursi and A. Al Hinai, “Coordinated Frequency Control Strategy for an Islanded Microgrid with Demand Side Management Capability,” *IEEE Transactions on Energy Conversion*, vol. PP, no. 99, pp. 1–12, 2017.
- [32] L. Fabietti, T. T. Gorecki, E. Namor, F. Sossan, M. Paolone and C. N. Jones, “Dispatching active distribution networks through electrochemical storage systems and demand side management,” *2017 IEEE Conference on Control Technology and Applications (CCTA)*, pp. 1241–1247, 2017.
- [33] Baidyanath Bag and Tripta Thakur, “A Utility Initiative based Method for Demand Side Distribution Network Containing Voltage Regulated,” *2016 International Conference on Electrical Power and Energy Systems (ICEPES)*, pp. 52–57, 2016.
- [34] J. Zhuang, G. Shen, J. Yu, T. Xiang and X. Wang, “Micro-grid Energy Storage Location and Sizing Optimization Method Based on Demand Response,” *2016 International Conference on Intelligent Transportation, Big Data & Smart City (ICITBS)*, pp. 517–520, 2017.
- [35] K. S. Reddy, L. Panwar, B. K. Panigrahi, R. Kumar and H. Yu, “Demand side management with consumer clusters in cyber-physical smart distribution system considering price-based and reward-based scheduling programs,” *IET Cyber-Physical Systems: Theory & Applications*, vol. 2, no. 2, pp. 75–83, 2017.
- [36] M. Ghorbanian, H. Narimani and G. Reza Yousefi, “Billing Mechanism Design in an Autonomous Demand Side Management in a Smart,” *2017 Iranian Conference on Electrical Engineering (ICEE)*, pp. 1284–1290, 2017.
- [37] A. Esmat, P. Pinson and J. Usaola, “Decision Support Program for Congestion Management using Demand Side Flexibility,” *2017 IEEE Manchester PowerTech*, pp. 1–6, 2017.
- [38] X. Tang and J. V Milanovi, “Assessment of the Impact of Demand Side Management on Power System Small Signal Stability,” *2017 IEEE Manchester PowerTech*, pp. 1–6, 2017.
- [39] N. Blaauwbroek, P. Nguyen and H. Sloopweg, “Applying Demand Side Management using a Generalised Three Phase Grid Supportive Approach,” *2017 IEEE International Conference on Environment and Electrical Engineering and 2017 IEEE Industrial and Commercial Power Systems Europe (EEEIC / I&CPS Europe)*, pp. 1–6, 2017.

- [40] M. Kiaee, A. J. Cruden and S. M. Sharkh, "Demand side management of electric vehicle car parks to increase integrated solar power capacity within an existing radial distribution network," *6th Hybrid and Electric Vehicles Conference (HEVC 2016)*, pp. 1–6, 2016.
- [41] Z. Wang, F. Li and Z. Li, "Active Household Energy Storage Management in Distribution Networks to Facilitate Demand Side Response," *2012 IEEE Power and Energy Society General Meeting*, pp. 1–6, 2012.
- [42] C. Wu, H. Mohsenian-Rad, J. Huang and A. Y. Wang, "Demand Side Management for Wind Power Integration in Microgrid Using Dynamic Potential Game Theory," *2011 IEEE GLOBECOM Workshops (GC Wkshps)*, pp. 1199–1204, 2011.
- [43] V. Prema, K. U. Rao and A. S. Closepet, "A Novel Predictive DSM Strategy to Match Power Outage Pattern for Optimal Cost with Solar and Diesel Power," *2014 IEEE Innovative Smart Grid Technologies - Asia (ISGT ASIA)*, pp. 377–382, 2014.
- [44] H. Wei, H. Zijun, Fengli, T. Hongliang and Z. Li, "Reliability evaluation of Microgrid with PV-WG hybrid system," *2011 4th International Conference on Electric Utility Deregulation and Restructuring and Power Technologies (DRPT)*, pp. 1629–1632, 2011.
- [45] P. Alinezhad, O. Z. Bakhoda and M. B. Menhaj, "Optimal DG placement and capacity allocation using intelligent algorithms," *2015 4th Iranian Joint Congress on Fuzzy and Intelligent Systems (CFIS)*, pp. 1–8, 2015.
- [46] Minnan Wang and Jin Zhong, "Islanding of systems of distributed generation using optimization methodology," *2012 IEEE Power and Energy Society General Meeting*, pp. 1–7, 2012.
- [47] S. C. Reddy, P. V. N. Prasad and A. J. Laxmi, "Reliability improvement of distribution system by optimal placement of DGs using PSO and neural network," *2012 International Conference on Computing, Electronics and Electrical Technologies (ICCEET)*, pp. 156–162, 2012.
- [48] A. K. Singh and S. K. Parida, "Selection of load buses for DG placement based on loss reduction and voltage improvement sensitivity," *2011 International Conference on Power Engineering, Energy and Electrical Drives*, pp. 1–6, 2011.
- [49] Israfil Hussain and Anjan Kumar Roy, "Optimal distributed generation allocation in distribution systems employing modified artificial bee colony algorithm to reduce losses and improve voltage profile," *IEEE-International Conference On Advances In Engineering, Science And Management (ICAESM -2012)*, pp. 565–570, 2012.

- [50] A. Esmat, A. Magdy, W. ElKhattam and A. M. ElBakly, "A novel Energy Management System using Ant Colony Optimization for micro-grids," *2013 3rd International Conference on Electric Power and Energy Conversion Systems*, pp. 1–6, 2013.
- [51] H. Yassami, A. Moeini, S. M. R. Rafiei, A. Darabi and A. Bagheri, "Optimal distributed generation planning considering reliability , cost of energy and power loss," *Scientific Research and Essays*, vol. 6, no. 9, pp. 1963–1976, 2011.
- [52] P. Phonrattanasak, "Optimal Placement of Wind Farm on the Power System Using Multiobjective Bees Algorithm," *Proc. World Congr. Eng. 2011*, vol. 2, no. 3, pp. 1–5, 2011.
- [53] R. Sayed, Y. G. Hegazy and M. A. Mostafa, "Modeling of Photovoltaic Based Power Stations for Reliability Studies Using Markov Chains," *2013 International Conference on Renewable Energy Research and Applications (ICRERA)*, pp. 667–673, 2013.
- [54] H. Shayeghi, M. Moradzadeh, Y. Hashemi, M. Saif and L. Vandeveld, "Wind-PV-Storage Optimal Environomic Design Using Multi- objective Artificial Bee Colony," *2015 IEEE PES Asia-Pacific Power and Energy Engineering Conference (APPEEC)*, pp. 1–5, 2015.
- [55] G. B. Shrestha and L. Goel, "A study on optimal sizing of stand-alone photovoltaic stations," *IEEE Transactions on Energy Conversion*, vol. 13, no. 4, pp. 373–378, 1998.
- [56] N. D. Kaushika, N. K. Gautam and K. Kaushik, "Simulation model for sizing of stand-alone solar PV system with interconnected array," *Sol. Energy Mater. Sol. Cells*, vol. 85, no. 4, pp. 499–519, 2005.
- [57] S. Elsaiah, M. Benidris and J. Mitra, "Reliability improvement of power distribution system through feeder reconfiguration," *2014 International Conference on Probabilistic Methods Applied to Power Systems (PMAPS)*, pp. 1–6, 2014.
- [58] C. Venu, Y. Rifonnoeu, S. Bacha and Y. Baghzouz, "Battery Storage System sizing in distribution feeders with distributed photovoltaic systems," *2009 IEEE Bucharest PowerTech*, pp. 1–5, 2009.
- [59] M. M. H. Bhuiyan and M. A. Asgar, "Sizing of a stand-alone photovoltaic power system at Dhaka," *Renew. Energy*, vol. 28, no. 6, pp. 929–938, 2003.

- [60] F. Abbasi and S. M. Hosseini, "Optimal DG allocation and sizing in presence of storage systems considering network configuration effects in distribution systems," *IET Generation, Transmission & Distribution*, vol. 10, no. 3, pp. 617–624, 2016.
- [61] B. Esmailnezhad and H. Shayeghi, "Simultaneous Distribution Network Reconfiguration and DG Allocation for Loss Reduction by Invasive Weed Optimization Algorithm," *2013 Smart Grid Conference (SGC)*, pp. 166–172, 2013.
- [62] F. S. Abu-Mouti and M. E. El-Hawary, "Sizing in Distribution Systems via Artificial Bee Colony Algorithm," *IEEE Transactions on Power Delivery*, vol. 26, no. 4, pp. 2090–2101, 2011.
- [63] L. S. M. Guedes, A. C. Lisboa, D. A. G. Vieira and R. R. Saldanha, "A Multiobjective Heuristic for Reconfiguration of the Electrical Radial Network," *IEEE Transactions on Power Delivery*, vol. 28, no. 1, pp. 311–319, 2013.
- [64] N. H. Shamsudin, M. S. S. M. Basir, A. R. Abdullah, M. F. Sulaima and E. F. Shair "Losses Minimization in Network Reconfiguration for Fault Restoration Via A Uniform Crossover of Genetic Algorithm Losses Minimization in Network Reconfiguration for Fault Restoration Via A Uniform Crossover of Genetic Algorithm," *2015 International Symposium on Technology Management and Emerging Technologies (ISTMET)*, pp. 330–334, 2015.
- [65] E. Moazami, M. Z. A. A. Kadir, H. Hizam, M. Izadi and M. Mirzaei, "Optimal Penalty Method in Distribution Service Restoration using Genetic Algorithm," *2013 IEEE 7th International Power Engineering and Optimization Conference (PEOCO)*, pp. 397–401, 2013.
- [66] E. G. Carrano, G. P. Silva, E. P. Cardoso and R. H. C. Takahashi, "Subpermutation-Based Evolutionary Multiobjective Algorithm for Load Restoration in Power Distribution Networks," *IEEE Transactions on Evolutionary Computation*, vol. 20, no. 4, pp. 546–562, 2016.
- [67] F. Shariatzadeh, C. B. Vellaithurai, S. S. Biswas, R. Zamora and A. K. Srivastava, "Real-Time Implementation of Intelligent Reconfiguration Algorithm for Microgrid," *IEEE Transactions on Sustainable Energy*, vol. 5, no. 2, pp. 598–607, 2014.
- [68] Y. Kumar, B. Das and J. Sharma, "Genetic algorithm for supply restoration in distribution system with priority customers," *2006 International Conference on Probabilistic Methods Applied to Power*, pp. 1–7, 2006.
- [69] T. M. Khalil and A. V Gorpnich, "Reconfiguration for Loss Reduction of Distribution Systems Using Selective Particle Swarm Optimization," *International*

- Journal of Multidisciplinary Sciences and Engineering*, vol. 3, no. 6, pp. 16–21, 2012.
- [70] S. Fang and X. Zhang, “A Hybrid Algorithm of Particle Swarm Optimization and Tabu Search for Distribution Network Reconfiguration,” *Mathematical Problems in Engineering*, vol. 2016, pp. 1–7, 2016.
- [71] Y. Hong and S. Ho, “Determination of Network Configuration Considering Multiobjective in Distribution Systems Using Genetic Algorithms,” *IEEE Transactions on Power Systems*, vol. 20, no. 2, pp. 1062–1069, 2005.
- [72] V. Calderaro, A. Piccolo and P. Siano, “Maximizing DG Penetration in Distribution Networks by means of GA based Reconfiguration,” *2005 International Conference on Future Power Systems*, pp. 1–6, 2005.
- [73] B. Enacheanu, B. Raison, R. Caire, O. Devaux, W. Bienia and N. Hadjsaid, “Radial Network Reconfiguration Using Genetic Algorithm Based on the Matroid Theory,” *IEEE Transactions on Power Systems*, vol. 23, no. 1, pp. 186–195, 2008.
- [74] C. Shen, P. Kaufmann and M. Braun, “A New Distribution Network Reconfiguration and Restoration Path Selection Algorithm,” *2014 Power Systems Computation Conference*, pp. 1–6, 2014.
- [75] F. Hsu and M. Tsai, “A Multi-Objective Evolution Programming Method for Feeder Reconfiguration of Power Distribution System,” *13th International Conference on Intelligent Systems Application to Power Systems*, pp. 55–60, 2005.
- [76] Y. Hsiao and C. Chien, “Enhancement of Restoration Service in Distribution Systems Using a Combination Fuzzy – GA Method,” *IEEE Transactions on Power Systems*, vol. 15, no. 4, pp. 1394–1400, 2000.
- [77] N.H. Shamsudin, N.F. Omar, A.R. Abdullah, M.F. Sulaima, N.A. Abidullah and H.I. Jaafar, “An Improved Genetic Algorithm for Power Losses Minimization using Distribution Network Reconfiguration Based on Re-rank Approach,” *Research Journal of Applied Sciences, Engineering and Technology*, pp. 1029–1035, 2014.
- [78] L. T. Marques, D. S. Sanches, A. C. B. Delbem and J. B. A. London, “Methodology for service restoration in large-scale distribution systems with priority customers,” *IEEE PES Innovative Smart Grid Technologies*, pp. 1–6, 2014.
- [79] A. S. Bretas and A. G. Phadke, “Artificial Neural Networks in Power System Restoration,” *IEEE Trans. Power Deliv.*, vol. 18, no. 4, pp. 1181–1186, 2003.
- [80] Karen Nan Miu, Hsiao-Dong Chiang and R. J. McNulty, “Multi-Tier Service Restoration Through Network Reconfiguration and Capacitor Control for Large-

- Scale Radial Distribution Networks,” *IEEE Trans. Power Syst.*, vol. 15, no. 3, pp. 1001–1007, 2000.
- [81] Y. Kumar, B. Das and J. Sharma, “Multiobjective, Multiconstraint Service Restoration of Electric Power Distribution System With Priority Customers,” *IEEE Trans. Power Deliv.*, vol. 23, no. 1, pp. 261–270, 2008.
- [82] K. N. Miu, Hsiao-Dong Chiang and R. J. McNulty, “Multi-tier service restoration through network reconfiguration and capacitor control for large-scale radial distribution networks,” *21st International Conference on Power Industry Computer Applications. Connecting Utilities. PICA 99. To the Millennium and Beyond (Cat. No.99CH36351)*, pp. 153–159, 1999.
- [83] R. Hardowar, S. Rodriguez, R. Uosef, F. De Leon and D. Czarkowski, “Prioritizing the Restoration of Network Transformers using Distribution System Loading and Reliability Indices,” *IEEE Trans. Power Deliv.*, vol. 32, no. 3, pp. 1236–1243, 2017.
- [84] K. N. Miu, Hsiao-Dong Chiang and R. J. McNulty, “Multi-tier service restoration through network reconfiguration and capacitor control for large-scale radial distribution networks,” *21st International Conference on Power Industry Computer Applications*, pp. 153–159, 1999.
- [85] Y. Kumar, B. Das and J. Sharma, “Multiobjective, Multiconstraint Service Restoration of Electric Power Distribution System With Priority Customers,” *IEEE Trans. Power Deliv.*, vol. 23, no. 1, pp. 261–270, 2008.
- [86] W. De Soto, S. A. Klein and W. A. Beckman, “Improvement and validation of a model for photovoltaic array performance,” *Solar Energy*, vol. 80, pp. 78–88, 2006.
- [87] Q. Song and B. S. Chissom, “Fuzzy time series and its models,” *Fuzzy Sets Syst.*, vol. 54, pp. 269–277, 1993.
- [88] S. Chen and C. Hsu, “A new method to forecast enrollments using fuzzy time series,” *Int. J. Appl. Sci. Engg.*, pp. 234–244, 2004.
- [89] M. H. F. Zarandi, A. Molladavoudi and M. H. Ali Beigi, “A new method for temperature prediction and the TAIFEX Forecasting based on fuzzy logical relationship and double Interval division,” *IEEM 2009 - IEEE Int. Conf. Ind. Eng. Eng. Manag.*, pp. 1543–1547, 2009.
- [90] L. W. Lee, L. H. Wang and S. M. Chen, “Temperature prediction and TAIFEX forecasting based on high-order fuzzy logical relationships and genetic simulated annealing techniques,” *Expert Syst. Appl.*, vol. 34, pp. 328–336, 2008.

- [91] V. Vamitha, M. Jeyanthi, S. Rajaram and T. Revathi, "Temperature Prediction Using Fuzzy Time Series and Multivariate Markov Chain," *International Journal of Fuzzy Mathematics and Systems*, vol. 2, no. 3, pp. 217–230, 2012.
- [92] J. Liu, S. Li and S. Jia, "A prediction model based on neural network and fuzzy Markov chain," *2008 7th World Congr. Intell. Control Autom.*, pp. 790–793, 2008.
- [93] S.T. Li and Y.C. Cheng, "A stochastic HMM-based forecasting model for fuzzy time series," *IEEE Trans. Syst. Man. Cybern. B. Cybern.*, vol. 40, no. 5, pp. 1255–1266, 2010.
- [94] Ruey-Chyn Tsaur, "A Fuzzy Time Series-Markov Chain Model with an Application to Forecast the Exchange Rate Between the Taiwan and US Dollar," *International Journal of Innovative Computing, Information and Control*, vol. 8, no. 7, pp. 4931–4942, 2012.
- [95] "Photovoltaic (PV) - Electrical Calculations." [Online]. Available: <http://myelectrical.com/notes/entryid/225/photovoltaic-pv-electrical-calculations>. [Accessed: 18-Apr-2016].
- [96] P. Arjyadhara, Ali S. M. and J. Chitralekha, "Analysis of Solar PV cell Performance with Changing Irradiance and Temperature," *Int. J. Eng. Comput. Sci.*, vol. 2, no. 1, pp. 214–220, 2013.
- [97] J. A. Duffie and W. A. Beckman, "Solar Engineering of Thermal Processes," *4th ed.*, 2013.
- [98] Key Features and Product Certificates, "CS6X-310," 2009.
- [99] A. Sankarakrishnan and R. Billinton, "Sequential Monte Carlo Simulation for Composite Power System Reliability Analysis with Time Varying Loads," *IEEE Transactions on Power Systems*, vol. 10, no. 3, pp. 1540–1545, 1995.
- [100] H. A. O. Jing, L. I. U. Dawei, L. I. Zhenxin, C. Zilai and K. Lingguo, "Energy Procedia Power System Load Forecasting Based on Fuzzy Clustering and Gray Target Theory," *2012 International Conference on Future Energy, Environment, and Materials*, pp. 1852–1859, 2012.
- [101] A. S. Carpinteiro, R. C. Leme, A. C. Zambroni, D. Souza, C. A. M. Pinheiro and E. M. Moreira, "Long-term load forecasting via a hierarchical neural model with time integrators," *Electric Power Systems Research*, vol. 77, pp. 371–378, 2007.
- [102] Y. Aslan, S. Yavasca and C. Yasar, "Long Term Electric Peak Load Forecasting of Kutahya Using Different Approaches," *6th International Conference on TPE (ICTPE-2010)*, pp. 191–195, 2011.

- [103] J. Song, V. Krishnamurthy, A. Kwasinski and R. Sharma, “Development of a Markov Chain Based Energy Storage Model for Power Supply Availability Assessment of Photovoltaic Generation Plants,” *IEEE Transactions on Sustainable Energy*, vol. 4, no. 2, pp. 491–500, 2013.
- [104] J. N. Morse, “Reducing the size of the nondominated set: Pruning by clustering,” *Comput. Oper. Res.*, vol. 7, no. 1–2, pp. 55–66, 1980.

|

Vitae

Name	:Md. Ilius Hasan Pathan
Nationality	:Bangladeshi
Date of Birth	:2/12/1988
Email	:pmilius2501@gmail.com
Address	:Bogra, Dhaka, Bangladesh
Academic Background	:Obtained B.Sc. degree in Electrical and Electronic Engineering from Rajshahi University of Engineering & Technology (RUET), Rajshahi, Bangladesh in 2011. He has completed M.Sc. in Electrical Power from Electrical Engineering Department at King Fahd University of Petroleum and Minerals in December 2017.
Research Interests	:Power System Operation, Control, and Optimization, Renewable Energy, Application of Artificial Intelligence in Power Systems, Demand Side Management, Control and Reliability Assessment of Microgrid, Smart Grid Technologies and their Impact on Grid operation.

APPENDIX A

Branch Number	Failure Rate	Repair Rate
1	0.0005/8760	480/8760
2	0.0009/8760	480/8760
3	0.001/8760	469/8760
4	0.0012/8760	470/8760
5	0.002/8760	450/8760
6	0.0026/8760	455/8760
7	0.0011/8760	460/8760
8	0.0006/8760	365/8760
9	0.0015/8760	440/8760
10	0.0028/8760	442/8760
11	0.0015/8760	430/8760
12	0.0015/8760	335/8760
13	0.0028/8760	345/8760
14	0.0029/8760	431/8760
15	0.003/8760	430/8760
16	0.0017/8760	433/8760
17	0.001/8760	329/8760
18	0.0018/8760	340/8760
19	0.0022/8760	356/8760
20	0.0025/8760	450/8760
21	0.003/8760	341/8760
22	0.003/8760	378/8760
23	0.0034/8760	380/8760
24	0.0032/8760	400/8760
25	0.0011/8760	401/8760
26	0.0014/8760	411/8760
27	0.0028/8760	370/8760
28	0.0029/8760	392/8760
29	0.0026/8760	396/8760
30	0.0026/8760	382/8760
31	0.0021/8760	360/8760
32	0.0027/8760	367/8760

APPENDIX B

Tie Set Calculation of Each Bus point of IEEE 33 Bus Distribution Network (On State of All Branch Number of a Tie Set Results That Bus On State, Off State of One or More Branches of a Tie Set Results That Bus Off State)	
Tie Set Number	Branch Number
Tie Set for Bus 2	[1]
Tie Set for Bus 3	[1, 2]
Tie Set for Bus 4	[1, 2, 3]
Tie Set for Bus 5	[1, 2, 3, 4]
Tie Set for Bus 6	[1, 2, 3, 4, 5]
Tie Set for Bus 7	[1, 2, 3, 4, 5, 6]
Tie Set for Bus 8	[1, 2, 3, 4, 5, 6, 7]
Tie Set for Bus 9	[1, 2, 3, 4, 5, 6, 7, 8]
Tie Set for Bus 10	[1, 2, 3, 4, 5, 6, 7, 8, 9]
Tie Set for Bus 11	[1, 2, 3, 4, 5, 6, 7, 8, 9, 10]
Tie Set for Bus 12	[1, 2, 3, 4, 5, 6, 7, 8, 9, 10, 11]
Tie Set for Bus 13	[1, 2, 3, 4, 5, 6, 7, 8, 9, 10, 11, 12]
Tie Set for Bus 14	[1, 2, 3, 4, 5, 6, 7, 8, 9, 10, 11, 12, 13]
Tie Set for Bus 15	[1, 2, 3, 4, 5, 6, 7, 8, 9, 10, 11, 12, 13, 14]
Tie Set for Bus 16	[1, 2, 3, 4, 5, 6, 7, 8, 9, 10, 11, 12, 13, 14, 15]
Tie Set for Bus 17	[1, 2, 3, 4, 5, 6, 7, 8, 9, 10, 11, 12, 13, 14, 15, 16]
Tie Set for Bus 18	[1, 2, 3, 4, 5, 6, 7, 8, 9, 10, 11, 12, 13, 14, 15, 16, 17]
Tie Set for Bus 19	[1, 18]
Tie Set for Bus 20	[1, 18, 19]
Tie Set for Bus 21	[1, 18, 19, 20]
Tie Set for Bus 22	[1, 18, 19, 20, 21]
Tie Set for Bus 23	[1, 2, 22]
Tie Set for Bus 24	[1, 2, 22, 23]
Tie Set for Bus 25	[1, 2, 22, 23, 24]
Tie Set for Bus 26	[1, 2, 3, 4, 5, 25, 26, 27]
Tie Set for Bus 27	[1, 2, 3, 4, 5, 25, 26, 27, 28]
Tie Set for Bus 28	[1, 2, 3, 4, 5, 25, 26, 27, 28]
Tie Set for Bus 30	[1, 2, 3, 4, 5, 25, 26, 27, 28, 29]
Tie Set for Bus 31	[1, 2, 3, 4, 5, 25, 26, 27, 28, 29, 30]
Tie Set for Bus 32	[1, 2, 3, 4, 5, 25, 26, 27, 28, 29, 30, 31]
Tie Set for Bus 33	[1, 2, 3, 4, 5, 25, 26, 27, 28, 29, 30, 31, 32]